

Low-Rank Modeling and Its Applications in Image Analysis

Xiaowei Zhou, The Hong Kong University of Science and Technology

Can Yang, Yale University

Hongyu Zhao, Yale University

Weichuan Yu, The Hong Kong University of Science and Technology

Low-rank modeling generally refers to a class of methods that solve problems by representing variables of interest as low-rank matrices. It has achieved great success in various fields including computer vision, data mining, signal processing and bioinformatics. Recently, much progress has been made on low-rank modeling in both theories and applications, such as exact low-rank matrix recovery via convex programming and matrix completion applied to collaborative filtering. These advances have brought more and more attentions to this topic. In this paper, we review recent progresses of low-rank modeling, state-of-the-art algorithms, and related applications in image analysis. We first give an overview to the concept of low-rank modeling and problems. Next, we summarize generic methods for low-rank matrix recovery and illustrate their advantages and limitations. Then, we introduce applications of low-rank modeling in the context of image analysis. Finally, we conclude with discussions and future research directions.

1. INTRODUCTION

In many research fields, the data sets to be analyzed often have high dimensionality, which brings great challenges to data analysis. Such examples include videos in computer vision, documents in natural language processing, customers' records in recommender systems, and genomics data in bioinformatics.

Fortunately, the high-dimensional data in many problems often lie in a subspace with limited dimensions. Mathematically, if we represent each observation by a vector $\mathbf{d}_i \in \mathbb{R}^m$ and the entire data set by a big matrix $\mathbf{D} = [\mathbf{d}_1, \dots, \mathbf{d}_n]$, the low-dimensionality assumption can be translated into the following low-rank assumption: $\text{rank}(\mathbf{D}) \ll \min(m, n)$. A typical example in computer vision is Lambertian reflectance. If $\mathbf{d}_1, \dots, \mathbf{d}_n$ are n images of a Lambertian surface under various lighting conditions, which have been reshaped as vectors, it can be shown that $\text{rank}(\mathbf{D}) \leq 9$ [Basri and Jacobs 2003]. Another example is in signal processing, where \mathbf{d}_i represents a vector of signal intensities received by an antenna array at time point i . Then, $\text{rank}(\mathbf{D})$ will be limited by the number of signal sources. Interested readers are referred to [Markovsky 2012] for more low-rank examples.

In the real world, the raw data can hardly be perfectly low-rank due to the existence of noise. Therefore, the following model is more faithful to real situations

$$\mathbf{D} = \mathbf{X} + \mathbf{E}, \quad (1)$$

where \mathbf{X} corresponds to a low-rank component and \mathbf{E} corresponds to noise or error in measurement. Recovering the low-rank structure from noisy data turns to be the central task in many problems.

A conventional approach to finding the low-rank approximation is to solve the following optimization problem

$$\begin{aligned} \min_{\mathbf{X}} \quad & \|\mathbf{D} - \mathbf{X}\|_F^2, \\ \text{s.t.} \quad & \text{rank}(\mathbf{X}) \leq r, \end{aligned} \quad (2)$$

where $\|\mathbf{Y}\|_F = \sqrt{\sum_{ij} Y_{ij}^2}$ denotes the Frobenious norm of a matrix.¹ Solving such a minimization problem can be interpreted as seeking the optimal rank- r estimate of \mathbf{D} in a least-squares sense. According to the matrix approximation theorem [Eckart and Young 1936], the solution to (2) is given analytically by the singular value decomposition (SVD):

$$\mathbf{X}^* = \sum_{i=1}^r \sigma_i \mathbf{u}_i \mathbf{v}_i^T, \quad (3)$$

where $\{\mathbf{u}_i\}$, $\{\mathbf{v}_i\}$, and $\{\sigma_i\}$ for $i = 1, \dots, r$ are the left singular vectors, right singular vectors, and singular values of \mathbf{D} , respectively. The vectors $\mathbf{u}_1, \dots, \mathbf{u}_r$ also provide a set of orthonormal bases to represent a low-dimensional subspace that can best embed the data. This procedure corresponds to Principal Component Analysis (PCA) [Jolliffe 2002] in statistics.

While PCA is one of the most popular tools for data analysis because of the analytical solution in computation and the provable optimality under certain assumptions, it cannot address some difficult issues in real applications. Following are two common examples.

Recovery from a few entries. In many applications, we would like to recover a matrix from only a small number of observed entries. A typical example is that, in collaborative filtering for recommender systems, we hope to make predictions to customers' preference based on the information collected so far. The NetFlix problem [Koren et al. 2009] is a famous instance. The data is a big matrix \mathbf{D} with each entry $D_{ij} \in \{1, \dots, 5\}$ recording the rating of customer i for movie j . There are around 480K customers and 18K movies in the data set, but only 1.2% entries have values since each customer only rated about 200 movies on average. The problem is how to predict the ratings that have not been made yet based on the current observation. A popular solution is to assume that the rating matrix should be low-rank. This assumption is based on the fact that a subgroup of customers are likely to share a similar taste and their ratings to the movies will be highly correlated. Consequently, the rank of the rating matrix will be limited by the number of subgroups formed by the customers. Therefore, the problem turns to be recovering a low-rank matrix from a few entries. This problem is often called **Matrix Completion** (MC).

Recovery from gross errors. In some other applications, we have to recover a low-dimensional subspace from corrupted data. For example, the face images of a person may include glasses or shadows that occlude the true appearance. The classical PCA assumes independently and identically distributed (i.i.d.) Gassuan noise and adopts the sum of squared differences as the loss function, as shown in (2). Since the least-squares fitting is sensitive to outliers, the classical PCA can be easily corrupted by these gross errors. For example, the reconstructed face images would include artifacts caused by the glasses or shadows in the input images [De La Torre and Black 2003]. Recovering a subspace or low-rank matrix robustly in the presence of outliers has been a popularly-studied issue. This problem is often called **Robust Principal Component Analysis** (RPCA).

In recent years, many new techniques for low-rank matrix recovery have been proposed. In the following, we will introduce some representative works. Basically, they

¹In this paper, a matrix is denoted by a capital letter, e.g. \mathbf{Y} . An element and a column of \mathbf{Y} are denoted by Y_{ij} and \mathbf{y}_i , respectively.

can be divided into several categories based on their approaches to modeling the low-rank prior. The first approach is to minimize the rank of the unknown matrix subject to some constraints. The rank minimization is often achieved by convex relaxation. We call these methods as convex methods. The second approach is to factorize the unknown matrix as a product of two factor matrices. The rank of the unknown matrix is upper bounded by the ranks of the factor matrices. We call these methods as matrix factorization methods. The third approach is to explicitly include a low-rank constraint in the formulation. To make the constraint satisfied during optimization, these methods often use a greedy strategy that projects a result to the feasible set of the rank constraint. We call these methods as greedy methods.

The rest of this paper is organized as follows.² In Section 2, we will review the convex methods for low-rank matrix recovery. We shall introduce some typical models as well as the corresponding optimization algorithms to solve these models. In Section 3, we will introduce matrix factorization methods for low-rank matrix recovery. Notice that not all matrix factorization methods aim to recovery a low-rank matrix. For example, the results of nonnegative matrix factorization [Lee and Seung 1999] or dictionary learning [Tosic and Frossard 2011] are not necessarily low-rank. We will not discuss these methods here. In Section 4, we will introduce some other methods with greedy strategies. In Section 5, we will use synthesized experiments to illustrate the performances of the discussed algorithms. In Section 6, we will give a literature review of the applications of low-rank modeling in image processing and computer vision. Finally, we will conclude the paper with discussions in Section 7.

2. CONVEX METHODS

A direct approach to recovering a low-rank matrix is to minimize the rank of the matrix with certain constraints that make the estimated matrix consistent with original data. However, the rank minimization problem (RMP) is combinatorial and known to be NP-hard [Fazel 2002]. Therefore, convex relaxation is often used to make the minimization tractable. The most popular choice is to replace rank with the nuclear norm which is defined as

$$\|\mathbf{X}\|_* = \sum_{i=1}^r \sigma_i, \quad (4)$$

where $\sigma_1, \sigma_2, \dots, \sigma_r$ are singular values of \mathbf{X} and r is the rank of \mathbf{X} . The advantages of using the nuclear norm relaxation are mainly two-folds. Firstly, the nuclear norm is convex. Hence, the global optima of the relaxed problem can be achieved efficiently. Secondly, the nuclear norm is proven to be the tightest convex surrogate of rank [Fazel 2002]. It means that the nuclear norm is almost the best approximation to the rank operator in all convex functions. Moreover, the analogy between using the nuclear norm for low-rank matrix recovery and using the ℓ_1 -norm for sparse signal recovery was well established [Recht et al. 2010], and the exact recovery property has been proven for some low-rank matrix recovery models using the nuclear norm [Recht et al. 2010; Candès and Recht 2009; Candès et al. 2011]. Other relaxation techniques besides the nuclear norm can be found in [Fazel 2002; Mohan and Fazel 2010]. In the following, we will first introduce the convex models and then summarize the optimization algorithms.

²A conference version of this paper appeared in Proceedings of SPIE Defense, Security, and Sensing 2013 [Zhou and Yu 2013].

2.1. Matrix Completion

In matrix completion, missing values in a matrix are to be estimated given observed values $\{D_{ij} | ij \in \Omega\}$, where Ω denotes the set of observed entries. As discussed previously, the common assumption is that the matrix should be low-rank. To solve the problem, the following optimization problem is often considered:

$$\begin{aligned} \min_{\mathbf{X}} \quad & \text{rank}(\mathbf{X}), \\ \text{s.t.} \quad & \mathcal{P}_{\Omega}(\mathbf{X}) = \mathcal{P}_{\Omega}(\mathbf{D}), \end{aligned} \quad (5)$$

In this paper, we use $\mathcal{P}_{\Omega}(\mathbf{X})$ to denote the operation of projecting matrix \mathbf{X} to the space of all matrices with nonzero elements restricted in Ω , i.e. $\mathcal{P}_{\Omega}(\mathbf{X})$ has the same values as \mathbf{X} for the entries in Ω and zero values for the entries outside Ω . The equality constraint in (5) means that the recovered matrix should coincide with the existing data.

As we discussed earlier, replacing rank with the nuclear norm can make the problem tractable. In some recent works [Candès and Recht 2009; Cai et al. 2010], the following convex problem is solved:

$$\begin{aligned} \min_{\mathbf{X}} \quad & \|\mathbf{X}\|_*, \\ \text{s.t.} \quad & \mathcal{P}_{\Omega}(\mathbf{X}) = \mathcal{P}_{\Omega}(\mathbf{D}), \end{aligned} \quad (6)$$

Most importantly, Candès and Recht [2009] theoretically proved that the solution of (6) can exactly recover the low-rank matrix as well as the true rank with high probability, if the following conditions are satisfied: The locations of the observed entries Ω are uniformly distributed and $|\Omega| \geq Cn^{1.2}r \log n$, where $|\Omega|$ is the number of observed entries, C is a positive constant, n is the matrix size, and r is the rank. The inequality means that the number of observed entries should be sufficiently large.

In real applications, the observed entries might be noisy, and the equality constraint in (6) will be too strict, resulting in over-fitting [Mazumder et al. 2010]. Therefore, the following relaxed form of (6) is often considered for matrix completion with noise [Candès and Plan 2010; Mazumder et al. 2010]:

$$\min_{\mathbf{X}} \quad \frac{1}{2} \|\mathcal{P}_{\Omega}(\mathbf{D} - \mathbf{X})\|_F^2 + \lambda \|\mathbf{X}\|_*, \quad (7)$$

where the parameter λ controls the rank of \mathbf{X} and the selection of λ should depend on the noise level [Candès and Plan 2010].

2.2. Robust Principal Component Analysis

Recently, convex programming has also been used to solve RPCA. The typical method is named sparse and low-rank decomposition [Candès et al. 2011], where a matrix \mathbf{D} is decomposed as a sum of a low-rank component \mathbf{X} and a sparse component \mathbf{E} by minimizing the rank of \mathbf{X} and the cardinality of \mathbf{E} simultaneously. The surprising message is that, under some mild assumptions, the low-rank matrix can be exactly recovered by the following convex program named Principal Component Pursuit (PCP) [Candès et al. 2011]:

$$\begin{aligned} \min_{\mathbf{X}, \mathbf{E}} \quad & \|\mathbf{X}\|_* + \lambda \|\mathbf{E}\|_1, \\ \text{s.t.} \quad & \mathbf{X} + \mathbf{E} = \mathbf{D}. \end{aligned} \quad (8)$$

Here, the nuclear norm $\|\mathbf{X}\|_*$ and the ℓ_1 -norm $\|\mathbf{E}\|_1$ are the convex surrogates of rank and cardinality, respectively. Candès et al. [2011] and Chandrasekaran et al. [2011] analyzed the conditions for exact recovery. Briefly speaking, it has been proven in [Candès et al. 2011] that \mathbf{X} and \mathbf{E} can be exactly recovered with high probability if

the singular vectors of \mathbf{X} are not sparse and the nonzero entries of \mathbf{E} are sufficiently sparse with a random spatial distribution. Moreover, a theoretical choice of parameter λ is provided to make the exact recovery most likely.

The basic model in (8) has been extended to handle more scenarios such as Stable PCP that considers the Gaussian noise [Zhou et al. 2010], the outlier pursuit that incorporates group sparsity [Xu et al. 2012a], and the matrix recovery from compressive measurements [Wright et al. 2012]. In Stable PCP [Zhou et al. 2010], the equality constraint in (8) is relaxed to be $\|\mathbf{X} + \mathbf{E} - \mathbf{D}\|_F \leq \sigma$ to allow the existence of Gaussian noise. In implementation, the following problem is solved

$$\min_{\mathbf{X}, \mathbf{E}} \|\mathbf{X}\|_* + \lambda \|\mathbf{E}\|_1 + \frac{\mu}{2} \|\mathbf{X} + \mathbf{E} - \mathbf{D}\|_F^2, \quad (9)$$

where μ is a constant determined by the noise level.

2.3. Optimization Algorithms

The nuclear norm-based algorithms are based on the following theorem ([Cai et al. 2010, Theorem 2.1]):

THEOREM 2.1. *The solution to the following problem*

$$\min_{\mathbf{X}} \frac{1}{2} \|\mathbf{Z} - \mathbf{X}\|_F^2 + \lambda \|\mathbf{X}\|_* \quad (10)$$

is given by $\mathbf{X}^* = \mathcal{D}_\lambda(\mathbf{Z})$, where

$$\mathcal{D}_\lambda(\mathbf{Z}) = \sum_{i=1}^r (\sigma_i - \lambda)_+ \mathbf{u}_i \mathbf{v}_i^T, \quad (11)$$

r is the rank of \mathbf{Z} , $(x)_+ = \max(x, 0)$, and $\{\mathbf{u}_i\}$, $\{\mathbf{v}_i\}$ and $\{\sigma_i\}$ are the left singular vectors, the right singular vectors and the singular values of \mathbf{Z} , respectively.

In the literature, \mathcal{D}_λ refers to the singular value thresholding (SVT) operator [Cai et al. 2010], which serves as a basic ingredient in many convex algorithms for low-rank matrix recovery.

Based on Theorem 2.1, various algorithms have been developed for specific problems. Two most popular methods are the Proximal Gradient (PG) method [Moreau 1965] and the Augmented Lagrangian Method (ALM) [Bertsekas 1999], which are applicable to a variety of convex problems. The PG method is very useful to solve the norm-regularized maximum-likelihood problems such as the model in (7), whose energy function comprises a differentiable loss and a nonsmooth regularizer. Moreover, the PG method is often combined with the Nesterov method to accelerate the convergence [Nesterov 2007; Beck and Teboulle 2009]. Examples using the PG method include [Ji and Ye 2009; Mazumder et al. 2010; Toh and Yun 2010], etc. The ALM method is closely related to the Alternating Direction Method of Multipliers (ADMM) [Boyd 2010]. It provides a powerful framework to solve convex problems with equality constraints such as MC in (6) and PCP in (8). The algorithms used in [Lin et al. 2010; Candès et al. 2011] belong to this class. The details of PG and ALM will be given in the following subsections.

2.3.1. Proximal Gradient. In sparse learning problems, we usually consider the following optimization problem

$$\min_{\mathbf{X}} f(\mathbf{X}) + \lambda \mathcal{R}(\mathbf{X}), \quad (12)$$

where $f(\mathbf{X})$ usually denotes a differentiable loss function and $\mathcal{R}(\mathbf{X})$ corresponds to a convex regularizer which might be nonsmooth. For example, the matrix completion with noise in (7) uses $f(\mathbf{X}) = \|\mathcal{P}_\Omega(\mathbf{X} - \mathbf{D})\|_F^2$ and $\mathcal{R}(\mathbf{X}) = \|\mathbf{X}\|_*$.

If $f(\mathbf{X})$ is simply the sum of squared differences between \mathbf{X} and a given matrix, the problem in (12) is named the proximal problem [Moreau 1965], which can be solved analytically for many types of $\mathcal{R}(\mathbf{X})$. For example, if $\mathcal{R}(\mathbf{X})$ is the nuclear norm, the problem can be solved analytically based on Theorem 2.1.

The Proximal Gradient (PG) method [Moreau 1965] is usually used if $f(\mathbf{X})$ is differentiable but not in the form of sum of squares. In PG, a quadratic approximation to $f(\mathbf{X})$ is made around the previous estimate \mathbf{X}' in each iteration. Define

$$\begin{aligned} Q_\mu(\mathbf{X}, \mathbf{X}') &= f(\mathbf{X}') + \langle \nabla f(\mathbf{X}'), \mathbf{X} - \mathbf{X}' \rangle + \frac{\mu}{2} \|\mathbf{X} - \mathbf{X}'\|_F^2 + \lambda \mathcal{R}(\mathbf{X}), \\ &= \frac{\mu}{2} \|\mathbf{X} - [\mathbf{X}' - \frac{1}{\mu} \nabla f(\mathbf{X}')] \|_F^2 + \lambda \mathcal{R}(\mathbf{X}) + \text{const.}, \end{aligned} \quad (13)$$

where $\langle \cdot \rangle$ means the inner product and μ is a constant. It can be proven that [Beck and Teboulle 2009], if $f(\mathbf{X})$ is differentiable and convex with a Lipschitz continuous gradient satisfying

$$\|\nabla f(\mathbf{X}_1) - \nabla f(\mathbf{X}_2)\|_F \leq \mu \|\mathbf{X}_1 - \mathbf{X}_2\|_F, \quad (14)$$

(12) can be solved by repeatedly updating \mathbf{X} via

$$\begin{aligned} \mathbf{X}^{k+1} &= \arg \min_{\mathbf{X}} Q_\mu(\mathbf{X}, \mathbf{X}^k), \\ &= \arg \min_{\mathbf{X}} \frac{1}{2} \|\mathbf{X} - [\mathbf{X}^k - \frac{1}{\mu} \nabla f(\mathbf{X}^k)] \|_F^2 + \frac{\lambda}{\mu} \mathcal{R}(\mathbf{X}) \end{aligned} \quad (15)$$

with a convergence rate of $\mathcal{O}(1/k)$. It is easy to see that (15) is simply the proximal problem, which is often convenient to solve.

The Accelerated Proximal Gradient (APG) method uses the Nesterov method [Nesterov 1983] to accelerate the convergence of PG. Instead of making quadratic approximation around \mathbf{X}^k , APG makes the approximation at another point \mathbf{Y}^k , which is a linear combination of \mathbf{X}^k and \mathbf{X}^{k-1} . This modification will give a convergence rate of $\mathcal{O}(\frac{1}{k^2})$. Please refer to [Nesterov 2007; Beck and Teboulle 2009] for details. The APG method is summarized in Algorithm 1.

Algorithm 1 Accelerated Proximal Gradient (APG)

1. **Initialize:** $\mathbf{X}^0 = \mathbf{X}^{-1} \in \mathbb{R}^{m \times n}$, $t_0 = t_{-1} = 1$
 2. **repeat**
 3. $\mathbf{Y}^k = \mathbf{X}^k + \frac{t^{k-1}-1}{t^k}(\mathbf{X}^k - \mathbf{X}^{k-1})$
 4. $\mathbf{X}^{k+1} = \arg \min_{\mathbf{X}} Q_\mu(\mathbf{X}, \mathbf{Y}^k)$
 5. $t^{k+1} = \frac{1 + \sqrt{1 + 4(t^k)^2}}{2}$
 6. **until** convergence
-

The PG and APG methods have been intensively used to solve the matrix completion problem in (7), where the update step in (15) is solved via SVT. For example, the SOFT-IMPUTE algorithm in [Mazumder et al. 2010] solves (7) by iteratively updating \mathbf{X} :

$$\mathbf{X}^{k+1} = \mathcal{D}_\lambda(\mathcal{P}_\Omega(\mathbf{D}) + \mathcal{P}_{\Omega^\perp}(\mathbf{X}^k)) = \mathcal{D}_\lambda(\mathbf{X}^k - [\mathcal{P}_\Omega(\mathbf{X}^k) - \mathcal{P}_\Omega(\mathbf{D})]). \quad (16)$$

It is straightforward to find that (16) is equivalent to (15) with $\mu = 1$. Hence, the SOFT-IMPUTE algorithm can be interpreted as PG with fixed step length. The FPCA algorithm introduced in [Ma et al. 2011] is also based on PG with a continuation technique to accelerate the convergence. Ji and Ye [2009] and Toh and Yun [2010] also proposed different implementations of APG for matrix completion. Tomioka et al. [2010] proposed a Dual Augmented Lagrangian algorithm for matrix completion, which achieves super-linear convergence. It can be interpreted as a proximal method with the descending directions computed from the augmented Lagrangian of the dual problem.

2.3.2. Augmented Lagrangian Method. The Augmented Lagrangian Method (ALM) [Bertsekas 1999] is a classical tool to minimize a convex function with equality constraints. We will use PCP in (8) as an example to introduce this method.

To remove the constraint $\mathbf{X} + \mathbf{E} = \mathbf{D}$, a multiplier \mathbf{Y} is introduced and the augmented Lagrangian of (8) reads

$$L_\mu(\mathbf{X}, \mathbf{E}, \mathbf{Y}) = \|\mathbf{X}\|_* + \lambda \|\mathbf{E}\|_1 + \langle \mathbf{Y}, \mathbf{D} - \mathbf{X} - \mathbf{E} \rangle + \frac{\mu}{2} \|\mathbf{D} - \mathbf{X} - \mathbf{E}\|_F^2. \quad (17)$$

ALM alternates between the following two steps:

$$(\mathbf{X}^{k+1}, \mathbf{E}^{k+1}) = \arg \min_{\mathbf{X}, \mathbf{E}} L_\mu(\mathbf{X}, \mathbf{E}, \mathbf{Y}^k), \quad (18)$$

$$\mathbf{Y}^{k+1} = \mathbf{Y}^k + \mu(\mathbf{D} - \mathbf{X}^{k+1} - \mathbf{E}^{k+1}), \quad (19)$$

which are named primal minimization and dual ascent, respectively. For PCP, the primal minimization in (18) is difficult over \mathbf{X} and \mathbf{E} simultaneously. But if we fix one variable and minimize over the other one, the marginal optimization over \mathbf{X} (or \mathbf{E}) turns to be the nuclear norm (or ℓ_1 -norm) regularized proximal problem, which can be efficiently solved by SVT (or soft-thresholding [Boyd 2010]). Then, the \mathbf{X} -step and \mathbf{E} -step are repeated until convergence to solve (18).

Instead of exactly solving (18) before updating the dual variable \mathbf{Y} , a more efficient way is to update primal variables \mathbf{X} and \mathbf{E} for only one iteration [Lin et al. 2010; Candès et al. 2011]. This is named the Inexact Augmented Lagrangian Method (IALM), a special case of the Alternating Direction Method of Multipliers (ADMM) [Boyd 2010]. The method is summarized in Algorithm 2. It can be proven that the sequences $\{\mathbf{X}^k\}$ and $\{\mathbf{E}^k\}$ will converge to an optimal solution of (8) [Lin et al. 2010; Boyd 2010].

Algorithm 2 Inexact Augmented Lagrangian Method (IALM) for PCP

1. **Initialize:** $\mathbf{E}^0 = \mathbf{Y}^0 = \mathbf{0}$
 2. **repeat**
 3. $\mathbf{X}^{k+1} = \arg \min_{\mathbf{X}} L_\mu(\mathbf{X}, \mathbf{E}^k, \mathbf{Y}^k) = \mathcal{D}_{\mu^{-1}}(\mathbf{D} - \mathbf{E}^k + \mu^{-1}\mathbf{Y}^k)$
 4. $\mathbf{E}^{k+1} = \arg \min_{\mathbf{E}} L_\mu(\mathbf{X}^{k+1}, \mathbf{E}, \mathbf{Y}^k) = \mathcal{S}_{\lambda\mu^{-1}}(\mathbf{D} - \mathbf{X}^{k+1} + \mu^{-1}\mathbf{Y}^k)$
 5. $\mathbf{Y}^{k+1} = \mathbf{Y}^k + \mu(\mathbf{D} - \mathbf{X}^{k+1} - \mathbf{E}^{k+1})$
 6. **until** convergence
-

ALM can also be applied to matrix completion in (6). In [Lin et al. 2010], the equality constraint $\mathcal{P}_\Omega(\mathbf{X}) = \mathcal{P}_\Omega(\mathbf{D})$ is replaced by $\mathbf{X} = \mathbf{D} + \mathbf{E}$ and $\mathcal{P}_\Omega(\mathbf{E}) = \mathbf{0}$. The new constraint is equivalent to the original one, but the projection operator on \mathbf{X} has been removed. Then, the ALM is applied. In this way, minimizing the augmented Lagrangian over \mathbf{X} turns to be a proximal problem, which could be solved by SVT. ALM was also applied to solve the nonnegative matrix factorization problem for matrix completion [Xu et al. 2012b].

3. MATRIX FACTORIZATION

Instead of minimizing rank, another approach to modeling the low-rank property is by matrix factorization. Matrix factorization intends to decompose $\mathbf{X} \in \mathbb{R}^{m \times n}$ as a product of two matrices $\mathbf{X} = \mathbf{A}\mathbf{B}^T$, where $\mathbf{A} \in \mathbb{R}^{m \times r}$ and $\mathbf{B} \in \mathbb{R}^{n \times r}$. Using matrix factorization to model a low-rank matrix is based on the fact that

$$\text{rank}(\mathbf{A}\mathbf{B}^T) \leq \min(\text{rank}(\mathbf{A}), \text{rank}(\mathbf{B})). \quad (20)$$

Therefore, if r is small, \mathbf{X} has a small rank. Finally, the problem of recovering a low-rank matrix can be converted into estimating two factor matrices \mathbf{A} and \mathbf{B} . In this paper, we will discuss representative matrix-factorization methods in the context of low-rank matrix recovery. For a summary of matrix factorization methods, please refer to [Singh and Gordon 2008].

3.1. Matrix Factorization with Missing Values

Basically, the matrix factorization methods for matrix completion aim to solve the following optimization problem:

$$\min_{\mathbf{A}, \mathbf{B}} \frac{1}{2} \|\mathcal{P}_\Omega(\mathbf{D} - \mathbf{A}\mathbf{B}^T)\|_F^2. \quad (21)$$

Note that the above model is nonconvex and the dimension r of \mathbf{A} and \mathbf{B} have to be determined before computation.

3.1.1. Alternating Methods. A simple way to solve (21) is to alternatively estimate \mathbf{A} or \mathbf{B} by fixing the other one. Each subproblem turns to be a least-squares problem which admits a closed-form solution. Some matrix-factorization algorithms in computer vision literature fall in this category such as Shum et al. [1995] and Vidal and Hartley [2004]. However, as pointed out by Buchanan and Fitzgibbon [2005], this iterative approach converges very slowly due to the ambiguity of solutions. Suppose $(\hat{\mathbf{A}}, \hat{\mathbf{B}})$ is a solution pair of (21). $(\hat{\mathbf{A}}\mathbf{Q}, \hat{\mathbf{B}}\mathbf{Q})$ will also solve (21) for any orthogonal matrix $\mathbf{Q} \in \mathbb{R}^{r \times r}$. Moreover, the stability of the solution also depends on the sparsity and distribution of the observed set Ω .

Buchanan and Fitzgibbon [2005] developed a Damped Newton algorithm to solve the problem. The variables \mathbf{A} and \mathbf{B} are updated together based on the Newton algorithm with a damping factor. Compared with the first-order methods such as alternating least squares, the Newton-based algorithm would converge faster with better precision. However, they cannot handle large-scale problems due to the infeasibility of computing or even storing the Hessian matrix of a large number of variables.

To interpolate between the alternating least squares and the Newton algorithm, some works proposed to use hybrid algorithms. In the Wiberg algorithm [Okatani and Deguchi 2007], \mathbf{A} is updated via least squares while \mathbf{B} is updated by a Gauss-Newton step in each iteration. Later, the Wiberg algorithm was extended to a damped version to achieve better convergence [Okatani et al. 2011]. Chen [2008] proposed an algorithm similar to the Wiberg algorithm. The difference is that the updating of \mathbf{B} is done by the Levenberg-Marquadt algorithm and \mathbf{B} is constrained in $\{\mathbf{B} | \mathbf{B}^T \mathbf{B} = \mathbf{I}\}$. Interested readers can refer to [Okatani et al. 2011] for more details of the factorization algorithms in computer vision.

The matrix completion solver LMaFit [Wen et al. 2010] also adopted the alternating strategy to solve the following equivalent form of (21):

$$\begin{aligned} & \min_{\mathbf{A}, \mathbf{B}, \mathbf{Z}} \frac{1}{2} \|\mathbf{Z} - \mathbf{A}\mathbf{B}^T\|_F^2, \\ & \text{s.t. } \mathcal{P}_\Omega(\mathbf{Z}) = \mathcal{P}_\Omega(\mathbf{D}), \end{aligned} \quad (22)$$

where \mathbf{Z} is an auxiliary variable. Each step of updating \mathbf{A} , \mathbf{B} or \mathbf{Z} can be solved very efficiently. Additionally, LMaFit integrates a nonlinear successive over-relaxation scheme to accelerate the convergence of alternation. Although the formulation is non-convex without theoretical analysis, LMaFit achieved very competitive recovery accuracy and high efficiency in our experiments in Section 5.

3.1.2. Maximum Margin Matrix Factorization. An effective approach to addressing the ill-conditioning issue of the model in (21) is regularizing the parameters in estimation. A popular method in collaborative filtering is named Maximum Margin Matrix Factorization (MMMF) [Srebro et al. 2005], which penalizes the Frobenious norms of two factor matrices:

$$\min_{\mathbf{A}, \mathbf{B}} \frac{1}{2} \|\mathcal{P}_\Omega(\mathbf{D} - \mathbf{A}\mathbf{B}^T)\|_F^2 + \frac{\lambda}{2} (\|\mathbf{A}\|_F^2 + \|\mathbf{B}\|_F^2), \quad (23)$$

The idea is similar to using the squared ℓ_2 -norm in ridge regression to improve the stability of parameter estimation. Moreover, the following equality is established in [Srebro et al. 2005]

$$\|\mathbf{X}\|_* = \min_{\mathbf{A}, \mathbf{B}: \mathbf{X} = \mathbf{A}\mathbf{B}^T} \frac{1}{2} (\|\mathbf{A}\|_F^2 + \|\mathbf{B}\|_F^2), \quad (24)$$

which indicates the equivalence between MMMF in (23) and matrix completion via nuclear norm minimization in (7) [Srebro et al. 2005; Mazumder et al. 2010].

The problem (23) is solved as a semi-definite programming (SDP) problem in the original paper [Srebro et al. 2005]. Since SDP is not scalable to solve large-scale problems, a gradient-based method was later developed in [Rennie and Srebro 2005] to solve the model more efficiently.

3.1.3. Grassmannian Optimization. Another regularization strategy is to constrain \mathbf{A} and \mathbf{B} over the Grassmannian. The Grassmannian is a manifold composed of all r -dimensional subspaces in \mathbb{R}^m . If each subspace is represented by an orthogonal matrix composed of r basis vectors, the Grassmannian is $\{\mathbf{X} \in \mathbb{R}^{m \times r} | \mathbf{X}^T \mathbf{X} = \mathbf{I}\}$.

Keshavan et al. [2010] proposed an algorithm named OptSpace to solve the matrix completion problem in (21). It uses a rank- r approximation to the input matrix (with missing entries set to zero) as the initial low-rank matrix. In other words, it carries out SVD on the input matrix and uses the first r singular vectors as the initial values for \mathbf{A} and \mathbf{B} . To avoid the initial singular vectors being too heavily dependent on several high-degree columns or rows in the input matrix, it adopts a “trimming” step to remove such columns or rows. The degree of a column or a row refers to the number of nonzero entries in the column or the row. Moreover, it was shown in the paper that the underlying rank r can be revealed from the distribution of singular values of the trimmed input matrix. Next, \mathbf{A} and \mathbf{B} are updated in the “cleaning” step by using gradient descent on Grassmannian to minimize (21). Keshavan et al. [2010] proved that the reconstruction error of the initialized low-rank matrix after the trimming step is bounded and the exact recovery is of high probability after the cleaning step.

The SET algorithm developed in [Dai and Milenkovic 2010] is similar to OptSpace. The difference is that SET only updates the column space \mathbf{A} over Grassmannian while estimating \mathbf{B} by least squares in each iteration. Moreover, an additional step named

subspace transfer was introduced in SET to avoid the algorithm being trapped at local minima. Boumal and Absil [2011] developed an algorithm named RTRMC on Grassmannian with a Riemannian trust-region method.

3.2. Robust Matrix Factorization

Robust matrix factorization is to handle outliers in data, which can be regarded as the factorization approach towards RPCA. As mentioned before, the sensitivity of traditional methods to outliers is due to the squared loss used in (21), which penalizes large errors too much, resulting in biased fitting. To address this issue, a typical approach is to use more robust loss functions:

$$\min_{\mathbf{A}, \mathbf{B}} \sum_{ij} \rho(D_{ij} - [\mathbf{AB}^T]_{ij}), \quad (25)$$

where $[\mathbf{AB}^T]_{ij}$ denotes the entry ij of \mathbf{AB}^T and ρ is a robust loss function. For example, the Geman-McClure function defined as $\rho(x) = \frac{x^2}{2(1+x^2)}$ is adopted in [De La Torre and Black 2003]. To solve the optimization problem, alternating minimization is carried out, where \mathbf{A} and \mathbf{B} are updated iteratively by solving robust linear regression via iterative reweighted least squares or gradient-based methods. In [Ke and Kanade 2005], the ℓ_1 -penalty is used, and the problem is solved by alternating ℓ_1 -minimization.

3.3. Online Matrix Factorization

The demand of fast processing of streaming data (such as videos) stimulates many online algorithms for incremental estimation of the subspace. Generally, the following energy function of a subspace \mathbf{A} is minimized in each iteration when a new data vector \mathbf{d}_t arrives:

$$F^{(t)}(\mathbf{A}) = \min_{\mathbf{b}_t} \|\mathcal{P}_{\Omega_t}(\mathbf{d}_t - \mathbf{A}\mathbf{b}_t)\|_p^p, \quad (26)$$

where Ω_t denotes the set of observed entries in \mathbf{d}_t and $\|\cdot\|_p$ denotes the ℓ_p -norm. For example, the algorithm GROUSE proposed in [Balzano et al. 2010] uses the squared loss ($p = 2$) for matrix completion. In each iteration, \mathbf{b}_t is firstly solved via least squares, and \mathbf{A} is then updated via gradient descent of $F^{(t)}(\mathbf{A})$ over the Grassmannian.

The algorithm GRASTA introduced in [He et al. 2012] extends GROUSE to handle outliers for robust estimation by replacing the squared loss with the ℓ_1 -norm ($p = 1$). To solve the ℓ_1 -minimization problem in each iteration, the ADMM framework is used in GRASTA.

Recht and Ré [2011] proposed an efficient algorithm named JELLYFISH for large-scale matrix completion. It minimizes the energy function in (23) via incremental gradient descent, i.e. the variables are updated following an approximate gradient constructed from a sampling of matrix entries. Most importantly, JELLYFISH adopts a block matrix-partitioning scheme with a special sampling order to allow a parallel implementation of the algorithm on multiple cores to achieve a speed-up nearly proportional to the number of cores. In another work, Gemulla et al. [2011] adopted similar strategies for stochastic and parallel implementation.

3.4. Probabilistic Matrix Factorization

In this subsection, we shall briefly introduce a class of methods that treat low-rank matrix factorization from a probabilistic view.

3.4.1. Probabilistic PCA. Probabilistic PCA (PPCA) [Tipping and Bishop 1999] is a latent variable model which successfully formulates classical PCA [Jolliffe 2002;

Hotelling 1933] into the probabilistic framework. Let $\mathbf{d}_i \in \mathbb{R}^m$ be the i -th observed data point and $\mathbf{b}_i \in \mathbb{R}^r$ be the i -th latent variable in the latent space. PPCA assumes that \mathbf{d}_i is linearly related to \mathbf{b}_i by a matrix $\mathbf{A} \in \mathbb{R}^{m \times r}$:

$$\mathbf{d}_i = \mathbf{A}\mathbf{b}_i + \mathbf{e}_i, \quad (27)$$

where $\mathbf{e}_i \in \mathbb{R}^m$ denotes random noise, which follows a Gaussian distribution

$$\mathbf{e}_i \sim \mathcal{N}(\mathbf{0}, \beta^{-1}\mathbf{I}), \quad (28)$$

with β denoting the precision. Then, the likelihood of model (27) can be written as

$$\Pr(\mathbf{d}_i|\mathbf{A}, \mathbf{b}_i, \beta) = \mathcal{N}(\mathbf{d}_i|\mathbf{A}\mathbf{b}_i, \beta^{-1}\mathbf{I}). \quad (29)$$

To obtain the marginalized likelihood of \mathbf{A} , we need to integrate out \mathbf{b}_i :

$$\Pr(\mathbf{d}_i|\mathbf{A}, \beta) = \int \Pr(\mathbf{d}_i|\mathbf{A}, \mathbf{b}_i, \beta)\Pr(\mathbf{b}_i)d\mathbf{b}_i, \quad (30)$$

in which a prior distribution of \mathbf{b}_i has to be specified. PPCA adopts a zero mean and unit covariance Gaussian distribution as the prior. Then, the integration in (30) reads

$$\Pr(\mathbf{d}_i|\mathbf{A}, \beta) = \mathcal{N}(\mathbf{0}, \mathbf{A}\mathbf{A}^T + \beta^{-1}\mathbf{I}). \quad (31)$$

By further assuming the independence of data points, the likelihood of the full data is given by

$$\Pr(\mathbf{D}|\mathbf{A}, \beta) = \prod_{i=1}^n \Pr(\mathbf{d}_i|\mathbf{A}, \beta). \quad (32)$$

Finally, the matrix \mathbf{A} can be estimated by maximizing the above likelihood function. The maximum likelihood estimate (MLE) can be obtained analytically as

$$\hat{\mathbf{A}} = \mathbf{U}_r(\Lambda_r - \beta^{-1}\mathbf{I})^{1/2}\mathbf{Q}, \quad (33)$$

where the columns of $\mathbf{U}_r \in \mathbb{R}^{m \times r}$ are given by the r eigenvectors of the covariance matrix $\mathbf{D}^T\mathbf{D}$ corresponding to the r largest eigenvalues $\lambda_1, \dots, \lambda_r$, Σ_r is a diagonal matrix with the diagonal elements being $\lambda_1, \dots, \lambda_r$, and \mathbf{Q} is an arbitrary $r \times r$ orthogonal matrix. As a result, the column space of $\hat{\mathbf{A}}$ is identical to the subspace spanned by the principal components derived from the classical PCA.

The MLE of the noise variance is given by

$$\beta^{-1} = \frac{1}{n-r} \sum_{i=r+1}^n \lambda_i, \quad (34)$$

which can be interpreted as the average variance of the rest dimensions.

An advantage of probabilistic formulation of PCA is that it can be very helpful to automatically choose r by seeking a Bayesian approach [Bishop 1999]. Consider an independent Gaussian prior over each column of \mathbf{A} :

$$\Pr(\mathbf{A}|\boldsymbol{\gamma}) = \prod_{i=1}^r \left(\frac{\gamma_i}{2\pi}\right)^{m/2} \exp\left(-\frac{1}{2}\gamma_i\mathbf{a}_i^T\mathbf{a}_i\right). \quad (35)$$

where $\mathbf{a}_i \in \mathbb{R}^m$ is the i -th column of \mathbf{A} . Notice that the hyper-parameter γ_i controls the inverse variance of \mathbf{a}_i . When γ_i converges to a large value during the inference, it implies that the variance of \mathbf{a}_i should be small, and consequently the dimension spanned by \mathbf{a}_i can be switched off. An empirical Bayesian approach was used to find $\boldsymbol{\gamma}$, which is also known as automatic relevance determination (ARD) in the machine learning

literature [MacKay 1995; Bishop et al. 2006]. A well-known sparse machine learning model, relevance vector machines (RVM) [Tipping 2001], also adopted a similar technique to optimize the hyperparameters.

The estimation of \mathbf{b}_i can be treated similarly by integrating out \mathbf{A} , which is known as dual PPCA [Lawrence 2005].

3.4.2. Probabilistic Matrix Completion and RPCA. Probabilistic matrix factorization methods generally consider the following model to describe the observed data:

$$\mathbf{D} = \mathbf{A}\mathbf{B}^T + \mathbf{E}. \quad (36)$$

The probabilistic model can naturally handle missing values in matrix completion by only considering the likelihood over the observed entries

$$\Pr(\mathbf{D}|\Theta) = \prod_{ij \in \Omega} \Pr(D_{ij}|\Theta), \quad (37)$$

where Θ is the set of parameters and Ω is the set of observed entries.

A representative work is the Probabilistic Matrix Factorization (PMF) [Salakhutdinov and Mnih 2008b]. It assumes the following model:

$$\begin{aligned} A_{ij} &\sim \mathcal{N}(0, \gamma_a^{-1}), \\ B_{ij} &\sim \mathcal{N}(0, \gamma_b^{-1}), \\ E_{ij} &\sim \mathcal{N}(0, \beta^{-1}), \end{aligned} \quad (38)$$

where γ_a , γ_b and β are hyperparameters. If treating the hyperparameters as fixed values, we have the following posterior probability of \mathbf{A} and \mathbf{B}

$$\begin{aligned} \Pr(\mathbf{A}, \mathbf{B}|\mathbf{D}, \gamma_a, \gamma_b, \beta) &\propto \Pr(\mathbf{D}|\mathbf{A}, \mathbf{B}, \beta) \Pr(\mathbf{A}|\gamma_a) \Pr(\mathbf{B}|\gamma_b) \\ &= \prod_{ij \in \Omega} \mathcal{N}(D_{ij} | [\mathbf{A}\mathbf{B}^T]_{ij}, \beta^{-1}) \prod_{ij} \mathcal{N}(A_{ij} | 0, \gamma_a^{-1}) \prod_{ij} \mathcal{N}(B_{ij} | 0, \gamma_b^{-1}). \end{aligned} \quad (39)$$

After simple derivation, we can see that the maximum a posteriori (MAP) estimate of model (39) turns to be the solution of (23) with $\lambda = \gamma_a/\beta = \gamma_b/\beta$. This gives a probabilistic interpretation to MMMF. The Frobenius norm-regularization in MMMF corresponds to imposing Gaussian priors on \mathbf{A} and \mathbf{B} .

The advantage of probabilistic modeling is that the regularization parameters γ_a , γ_b and β needn't to be predefined. They can be automatically determined by treating them as variables, introducing priors on them and estimating them from the data [Salakhutdinov and Mnih 2008b]. Later, Salakhutdinov and Mnih [2008a] proposed a full Bayesian method for PMF and solved the model by Markov chain Monte Carlo (MCMC) sampling.

For RPCA, the prior on \mathbf{E} is changed. For instance, Wang et al. [2012] proposed Probabilistic Robust Matrix Factorization (PRMF) that used the Laplacian prior to model the error

$$\Pr(E_{ij}|\beta) = \left(\frac{\beta}{2}\right) \exp(-\beta|E_{ij}|). \quad (40)$$

Compared to the Gaussian prior, the Laplacian prior will encourage \mathbf{E} to be sparse and allow E_{ij} to have a large magnitude. The MAP estimate is given by the solution of the following optimization problem

$$\min_{\mathbf{A}, \mathbf{B}} \|\mathbf{D} - \mathbf{A}\mathbf{B}^T\|_1 + \lambda \|\mathbf{A}\|_F^2 + \lambda \|\mathbf{B}\|_F^2. \quad (41)$$

Notice that the Laplacian prior on the error term induces the ℓ_1 -penalty on the residue. One can see the connection between PRMF and PCP by comparing (41) with (24).

Babacan et al. [2012] proposed a Bayesian method to solve RPCA, in which the generative model is $\mathbf{D} = \mathbf{A}\mathbf{B}^T + \mathbf{E} + \mathbf{Z}$, where \mathbf{E} is a sparse matrix used to model outliers and \mathbf{Z} is a dense matrix used to model noise. Assuming Z_{ij} is i.i.d. Gaussian noise following $\mathcal{N}(0, \beta^{-1})$, the conditional probability of the observation is

$$\Pr(\mathbf{D}|\mathbf{A}, \mathbf{B}, \mathbf{E}, \beta) = \mathcal{N}(\mathbf{D}|\mathbf{A}\mathbf{B}^T + \mathbf{E}, \beta) \propto \exp\left(-\frac{\beta}{2}\|\mathbf{D} - \mathbf{A}\mathbf{B}^T - \mathbf{E}\|_F^2\right). \quad (42)$$

Moreover, the following priors were assumed

$$\begin{aligned} \Pr(\mathbf{E}|\boldsymbol{\alpha}) &= \prod_{ij} \mathcal{N}(E_{ij}|0, \alpha_{ij}^{-1}), \\ \Pr(\mathbf{A}|\boldsymbol{\gamma}) &= \prod_i \mathcal{N}(\mathbf{a}_i|\mathbf{0}, \gamma_i^{-1}\mathbf{I}), \\ \Pr(\mathbf{B}|\boldsymbol{\gamma}) &= \prod_i \mathcal{N}(\mathbf{b}_i|\mathbf{0}, \gamma_i^{-1}\mathbf{I}). \end{aligned} \quad (43)$$

Instead of using fixed values, the hyperparameters α_{ij} and γ_i were further modeled using Gamma priors. Finally, a variational algorithm was developed to estimate \mathbf{A} and \mathbf{B} as well as hyperparameters. Other probabilistic methods on robust matrix factorization include Lakshminarayanan et al. [2011]; Ding et al. [2011]; Wang and Yeung [2013], etc.

In probabilistic matrix factorization, the number of columns of \mathbf{A} or \mathbf{B} doesn't necessarily determine the rank of $\mathbf{A}\mathbf{B}^T$. It only serves as an upper bound and should be selected larger than the true rank. During the inference, the true rank will be determined automatically [Babacan et al. 2012]. The hierarchical modeling with hyperparameters plays an important role in the automatic determination. During the inference, some γ_i in (43) would converge to extremely large values, resulting in the corresponding columns being close to zero. The automatic "switch-off" of these columns driven by the data will determine the final rank of $\mathbf{A}\mathbf{B}^T$.

4. GREEDY METHODS

Greedy methods estimate a low-rank matrix under an explicit rank constraint. Basically, these methods require iterations, in which they iteratively seek a matrix with desired rank that best approximates the intermediate result. Since the rank constraint $\text{rank}(\mathbf{X}) \leq k$ defines a nonconvex set, the optimality of the solution cannot be guaranteed.

In [Jain et al. 2010], the following problem is considered:

$$\begin{aligned} \min_{\mathbf{X}} f(\mathbf{X}) &= \frac{1}{2} \|\mathcal{A}(\mathbf{X}) - \mathbf{b}\|_2^2, \\ \text{s.t. } \text{rank}(\mathbf{X}) &\leq r, \end{aligned} \quad (44)$$

where \mathcal{A} is a linear operator on \mathbf{X} . Notice that the matrix completion problem is a special case of (44). An algorithm named Singular Value Projection (SVP) was proposed in [Jain et al. 2010] to solve (44). It uses a projected gradient descent scheme which alternates between updating \mathbf{X} via gradient descent according to $f(\mathbf{X})$ and projecting the intermediate result to the set of rank- r matrices. By the matrix approximation theorem in (3), the projection is done by calculating the SVD of the matrix and keeping the r largest singular values. This procedure is similar to the proximal gradient method for nuclear norm minimization by replacing SVT with the low-rank projection. The

soft thresholding of singular values is applied in SVT, while the hard-thresholding of singular values is used in SVP. Therefore, SVP is analogous to the iterative hard thresholding algorithm in sparse coding [Blumensath and Davies 2009].

The ADMiRA algorithm introduced in [Lee and Bresler 2010] also intends to solve the problem in (44). Instead of using hard thresholding as in SVP, ADMiRA extends the CoSaMP algorithm [Needell and Tropp 2009] in compressive sensing to the matrix case. The matching pursuit-like [Mallat and Zhang 1993] scheme is used to stepwise select the basis vectors to construct the column space of \mathbf{X} which can minimize the function in (44). The SpaRCS algorithm proposed in [Waters et al. 2011] can be regarded as a counterpart of ADMiRA to solve the robust matrix recovery problem to handle the outlier issue.

The GoDec algorithm introduced in [Zhou and Tao 2011] uses the iterative hard thresholding method to solve the nonconvex formulation of RPCA:

$$\begin{aligned} \min_{\mathbf{X}, \mathbf{E}} \quad & \|\mathbf{D} - \mathbf{X} - \mathbf{E}\|_F^2 \\ \text{s.t.} \quad & \text{rank}(\mathbf{X}) \leq r, \\ & \|\mathbf{E}\|_0 \leq k. \end{aligned} \tag{45}$$

To minimize (45), GoDec estimates \mathbf{X} and \mathbf{E} alternatively. The two alternated steps correspond to the low-rank projection to estimate \mathbf{X} and the hard thresholding to estimate \mathbf{E} , respectively. To avoid the computation of SVD, GoDec uses a bilateral random projections scheme to compute the low-rank projection step.

5. NUMERICAL COMPARISON OF ALGORITHMS

A large number of algorithms have been proposed for low-rank matrix recovery and we have revisited some of them and summarized them into different categories. Table I gives an inexhaustive list of the algorithms. In this section, we would like to numerically illustrate the characteristics of different categories of algorithms. Since our paper does not focus on comprehensive comparisons, we only compare some selected solvers in each category. Also, we only test them on some synthesized data sets with typical settings. We encourage interested readers to refer to [Keshavan et al. 2009; Okatani et al. 2011; Michenková 2011] for more detailed comparisons.

More specifically, for matrix completion, we have tested APG [Toh and Yun 2010], ALM [Lin et al. 2010], LMatFit [Wen et al. 2010], OptSpace [Keshavan et al. 2010], GROUSE [Balzano et al. 2010] and VB [Babacan et al. 2012]. For RPCA, we have tested PCP [Candès et al. 2011], SPCP [Zhou et al. 2010], GoDec [Zhou and Tao 2011] and VB [Babacan et al. 2012]. All of the convex programs were implemented by the authors in MATLAB. For APG, we integrated the adaptive restart technique introduced in [O’Donoghue and Candès 2012], which can practically improve the convergence of APG. For ALM, we implemented the inexact version and adopted the varying penalty parameter scheme provided by Boyd [2010]. The SPCP algorithm in the original paper [Zhou et al. 2010] was solved by APG. Here, we implemented the block coordinate descent (BCD) algorithm to solve SPCP, i.e., we alternatively updated \mathbf{X} by SVT and updated \mathbf{E} by soft thresholding until convergence. In our experience, the efficiency of BCD is at least comparable to APG to solve the model in (9), while it is much simpler in implementation. For other algorithms, we used the MATLAB packages downloaded from the authors’ websites. For all algorithms, the default parameter settings in the original papers were used. The rank or the noise level is required in some algorithms and we simply provided their true values in the experiments.

The data sets are synthesized in the following way: The low-rank component is a square matrix generated by $\mathbf{L} = \mathbf{A}\mathbf{B}^T$, where both \mathbf{A} and \mathbf{B} are $m \times r$ random matrices with $r \ll m$. A_{ij} and B_{ij} are independently sampled from Gaussian distribution

Table I. Representative Low-Rank Matrix Recovery Algorithms.

Category	Algorithm & reference	Problem	Main techniques
Convex optimization	SVT [Cai et al. 2010]	MC	Proximal gradient (PG)
	FPCA [Ma et al. 2011]	MC	PG, approximate SVD
	SOFT-IMPUTE [Mazumder et al. 2010]	MC	PG, warm-start
	APG [Ji and Ye 2009; Toh and Yun 2010]	MC	Accelerated PG
	PCP [Candès et al. 2011]	RPCA	Augmented Lagrangian
	SPCP [Zhou et al. 2010]	RPCA	Accelerated PG
	ALM [Lin et al. 2010]	Both	Augmented Lagrangian
Matrix factorization	MMMF [Rennie and Srebro 2005]	MC	Gradient descent
	PMF [Salakhutdinov and Mnih 2008b]	MC	Gradient descent
	LMaFit [Wen et al. 2010]	MC	Alternated least squares
	OptSpace [Keshavan et al. 2010]	MC	Grassmannian
	SET [Dai and Milenkovic 2010]	MC	Grassmannian
	GROUSE [Balzano et al. 2010]	MC	Online algorithm
	JELLYFISH [Recht and Ré 2011]	MC	Stochastic & parallel
	GRASTA [He et al. 2012]	RPCA	Online algorithm
	BPRMF [Wang and Yeung 2013]	RPCA	Gibbs sampling
	VB [Babacan et al. 2012]	Both	Variational Bayes
Greedy projection	ADMIRA [Lee and Bresler 2010]	MC	Matching pursuit-like
	SVP [Jain et al. 2010]	MC	Hard thresholding
	GoDec [Zhou and Tao 2011]	RPCA	Hard thresholding

This list is inexhaustive. It only includes several representative algorithms in each category.

$\mathcal{N}(0, 1)$. L_{ij} is normalized to have unit variance. For matrix completion, the locations of missing values are defined by a binary matrix with entries independently sampled from a Binomial distribution $\mathcal{B}(1, \rho)$. For RPCA, the locations of outlier entries are defined by a binary matrix generated in the same way. The values of outlier entries are independently sampled from a uniform distribution $\mathcal{U}(-10, 10)$. Also, i.i.d. Gaussian noise is added to each entry with a variance σ^2 . The task is to recover L in the presence of missing values, outliers and noises.

To test the computational time, we simulated some problems with different sizes m and ranks r as shown in Table II and Table III. To test the recovery accuracy, we used two experiments. In the first experiment, we fixed the noise level σ and varied the proportion of missing or outlier entries ρ to test the recovery ability of the algorithms. In the second experiment, we fixed ρ and varied σ to see the robustness of algorithms against noise. We evaluate the accuracy by calculating the relative error defined as $\|L - \hat{X}\|_F / \|L\|_F$, where \hat{X} is the estimated matrix. The results are summarized as the curves shown in Figure 1 and Figure 2. Please note that the performance of an algorithm depends on many factors such as problem setting and parameter tuning. The results here are for the purpose of illustration instead of rigorous comparisons.

5.1. Matrix Completion

The computational time and accuracy for matrix completion are shown in Table II and Figure 1, respectively.

The convex methods (APG and IALM) are generally slower than the matrix factorization methods, since they have to perform SVD computation in each iteration. Partial SVD (only first several singular values are computed) is often used to accel-

Table II. Computational Time of Matrix Completion Algorithms.

Problem		Computational Time (sec)					
m	r	APG	IALM	LMatFit	OptSpace	GROUSE	VB
200	10	0.52	0.83	0.01	1.45	0.15	0.24
500	10	3.91	4.98	0.05	12.43	0.64	1.30
1000	10	22.17	33.60	0.24	57.42	2.06	4.11
1000	20	19.56	32.66	0.26	206.53	3.69	11.07
1000	50	23.42	36.64	0.46	1612.13	11.17	66.26

In this table, m is the matrix size and r is the matrix rank. The proportion of missing entries ρ and the noise level σ are fixed to be 0.5 and 0.1, respectively.

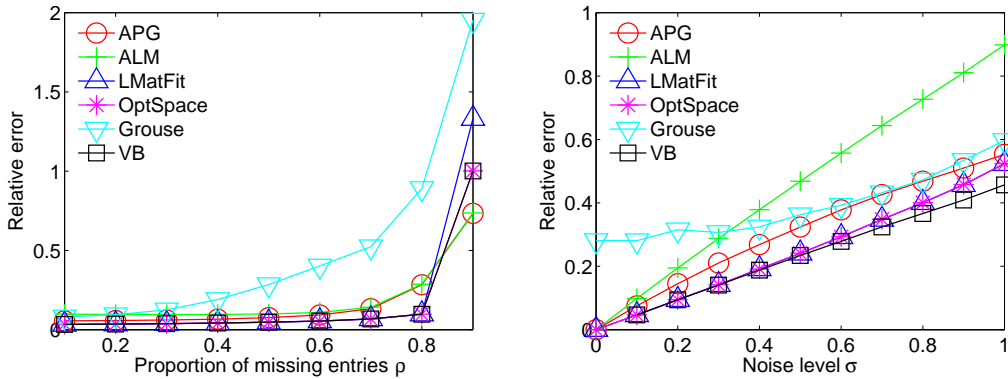


Fig. 1. Accuracy of the algorithms for matrix completion on simulated problems. In the left plot, the noise level is fixed with $\sigma = 0.1$ and the proportion of missing entries is varying. In the right plot, the proportion of missing entries is fixed with $\rho = 0.5$ and the noise level is varying.

erate the computation for large problems [Toh and Yun 2010; Lin et al. 2010]. In our experiments, we noticed that the speedup by partial SVD is limited when $m \leq 1000$.

Regarding accuracy, the convex methods achieved very stable performance under various situations. We can see that the relative error of the convex methods increases very smoothly as ρ increases and becomes the smallest compared to the other methods when $\rho \geq 0.9$. However, the accuracy of the convex methods is not the best in most of the cases. The reason is that, while convex relaxation can guarantee optimality in optimization, it may introduce bias into the model. For instance, the nuclear norm minimization will shrink the singular values of the recovered matrix. Consequently, the values of the recovered matrix are also shrunk towards zero. The unsatisfactory performance of IALM under large noise levels is due to the strict constraint in the corresponding model (6) which doesn't consider noise.

The factorization method LMatFit performed surprisingly well. It is much faster than the other methods with remarkable accuracy. However, when ρ is too large, its performance degrades dramatically. The possible reason is that it has no regularizer on the parameters. Hence, the estimation turns to be ill-conditioned when the observation is too sparse. Another drawback of LMatFit is that its performance depends on a predefined value of the matrix rank. In our test, we simply set the rank to be the true value, which is impractical in real applications. The Grassmanian method OptSpace achieved similar accuracy as LMatFit since their energy functions are similar. But the computation is slower. The online algorithm GROUSE is more efficient but less accurate than batch-based algorithms. Its greatest advantage is the ability to process data

Table III. Computational Time of RPCA Algorithms.

Problem		Computational Time (sec)			
m	r	PCP	SPCP	GoDec	VB
200	10	0.81	0.54	0.22	0.15
500	10	6.56	4.09	1.65	1.26
1000	10	37.48	25.57	7.17	5.21
1000	20	37.97	26.95	7.41	5.40
1000	50	39.73	29.13	8.38	6.19

In this table, m is the matrix size and r is the matrix rank. The proportion of outlier entries ρ and the noise level σ are both fixed as 0.1.

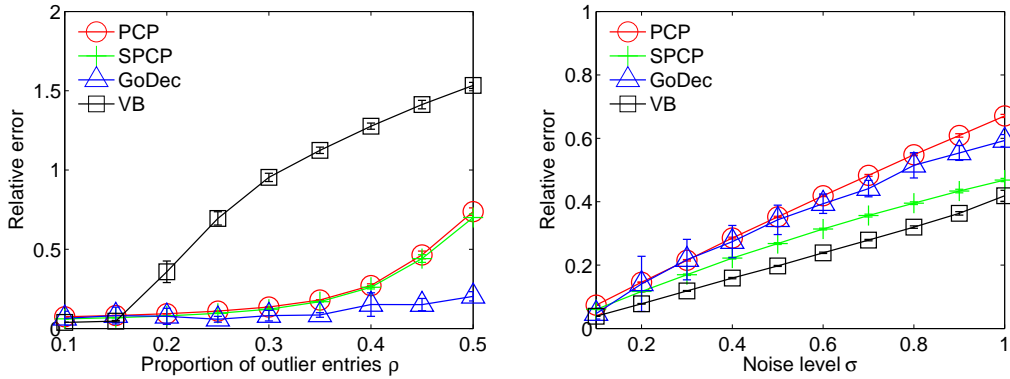


Fig. 2. Accuracy of RPCA algorithms on simulated problems with various missing ratios and noise levels. In the left plot, the noise level is fixed with $\sigma = 0.1$ and the proportion of outlier entries is varying. In the right plot, the proportion of outlier entries is fixed with $\rho = 0.1$ and the noise level is varying.

incrementally. The variational Bayesian method (VB) performs very well regarding both speed and accuracy. More importantly, no parameter tuning is required in VB.

5.2. RPCA

The computational time and accuracy for RPCA are shown in Table III and Figure 2, respectively.

Similar to the previous results for matrix completion, the convex methods (PCP and SPCP) are slower than the other methods. But the recovery accuracy of PCP and SPCP is very stable under all scenarios. Since PCP doesn't consider Gaussian noise, it has the lowest accuracy when σ is large.

The nonconvex method GoDec is very robust to outliers even when ρ is very large. The robustness is attributed to the ℓ_0 -penalty it adopts. However, this greedy algorithm may be affected by dense noise. We can see that the accuracy of GoDec is very good when σ is small but becomes worse than other methods when σ is larger. Moreover, GoDec requires the matrix rank and the cardinality of outliers to be predefined, both of which are unavailable in practice.

The VB method performs very well when ρ is small. But its performance decreases dramatically when $\rho > 15\%$. The possible reason is that VB adopts the alternating strategy for parameter estimation, which depends on initialization. When outliers are relatively dense, the initialization will be far away from the truth and the algorithm will converge to a local optimum.

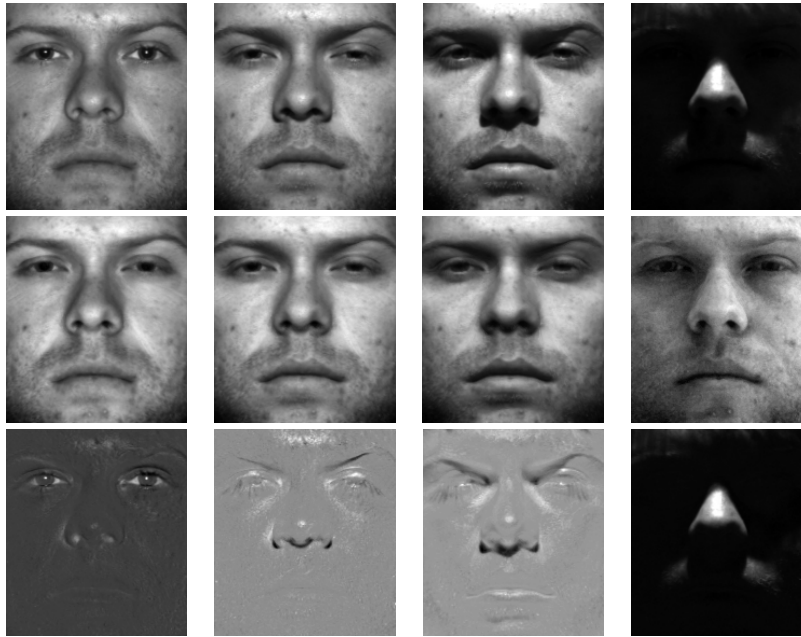


Fig. 3. Using RPCA to remove shadows and specularities in face images. From top to bottom are the original images, the low-rank components and the sparse components, respectively. We applied the PCP algorithm [Candès et al. 2011] to process a set of 64 face images of a subject from the Extended Yale Face Database B [Georghiades et al. 2001]. The face images were taken under different illuminations. The first four images are shown in the figure. Note that the displayed intensities in each image have been scaled to $[0, 255]$.

6. APPLICATIONS IN IMAGE ANALYSIS

Many objects of interest in image analysis can be modeled as low-rank matrices, such as the images of a convex lambertian surface under various illuminations [Basri and Jacobs 2003], dynamic textures changing periodically [Doretto et al. 2003], a group of active contours with similar shapes [Blake and Isard 2000], and multiple feature tracks on a rigid moving object [Vidal and Hartley 2004]. Intuitively, the low-dimensional subspace models the common patterns underlying the data. Hence, recovering the low-rank structure is critical to tasks such as background subtraction, face recognition, and segmentation. Below, we will introduce some typical applications based on the models we have discussed in the previous sections.

6.1. Face Recognition

The concept of low dimensionality has been used in face recognition for decades since the work by Sirovich and Kirby [1987]. PCA was applied on a set of face images to construct a face space and each face image can be characterized by a low-dimensional vector [Sirovich and Kirby 1987; Kirby and Sirovich 1990]. Later on, Turk and Pentland [1991] introduced the “eigenface” method for face recognition. The basic steps of using eigenfaces for face recognition include: (1) generating N eigenfaces by computing the first N eigenvectors of the matrix composed of a set of training images; (2) calculating the weight vector of an input image by projecting the image onto the space spanned by the N eigenfaces; and (3) determining whether the input image is a face image and which person the image belongs to according to the projection error and the weight vector. This is the earliest example of using low-rank approximation for face recognition.

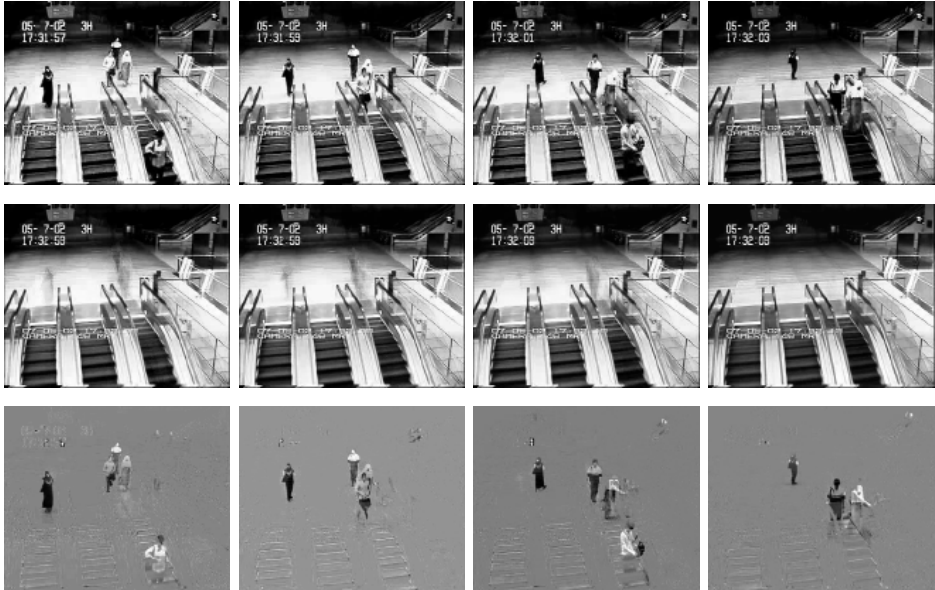


Fig. 4. Using RPCA for background subtraction. From top to bottom are the input images, the low-rank components (background) and the sparse components (foreground), respectively. We applied the PCP algorithm [Candès et al. 2011] on the subway station data set from [Li et al. 2004]. The data set is a surveillance video of a subway station including moving escalators in the background. We selected 200 frames to perform background subtraction and 4 frames to show the results in the figure.

The face images in real data sets are usually corrupted by various artifacts such as shadows, specularities and occlusions, which cannot be handled by classical PCA. Therefore, many approaches based on RPCA were proposed to process face images [De La Torre and Black 2003; Candès et al. 2011; Chen et al. 2012]. As illustrated in Figure 3, the local defects in face images could be removed as the sparse component, while the correct description of the person’s face could be obtained from the low-rank component. This procedure will improve the characterization of faces and boost the performance of recognition algorithms [Chen et al. 2012].

6.2. Background Subtraction

Background subtraction is to model the background in a video and detect the objects that stand out from the background. Similar to eigenfaces, PCA has been applied to model the background since the work “eigenbackground subtraction” [Oliver et al. 2000]. The basic idea is that the underlying background images of a video captured by a static camera should be unchanged except illumination variation. Therefore, the matrix composed of vectorized background images can be naturally modeled as a low-rank matrix. However, a set of training images without foreground object are required to generate the eigenbackground in traditional methods. The reason is that classical PCA can be easily corrupted by outliers. Consequently, clean background cannot be obtained without training images. Therefore, RPCA is desired [De La Torre and Black 2003]. As illustrated in [Candès et al. 2011], the PCP algorithm can recover the background images in the low-rank component and identify the foreground objects in the sparse component. Figure 4 gives an illustration. Notice that the background includes three moving escalators, which are clearly reconstructed in the low-rank component. This shows the appealing capability of low-rank modeling for background subtraction.

To achieve better accuracy for object detection, the contiguous property of foreground pixels can be modeled and integrated into RPCA by using Markov Random Fields or other smoothing techniques [Zhou et al. 2013b; Gao et al. 2012; Wang and Yeung 2013].

Similarly, the RPCA framework was used to segment the point trajectories in a video into two groups, which correspond to background and foreground, respectively [Cui et al. 2012]. The segmentation is based on the fact that the background motion in a video caused by camera motion should lie in a low-dimensional subspace.

6.3. Clustering and Classification

Another application of PCP is Low-Rank Representation (LRR) for subspace clustering [Liu et al. 2010]. In subspace clustering, the data points are assumed to be embedded in several low-dimensional subspaces, and the task is to find these subspaces and the membership of each data point in these subspaces. A popular method is spectral clustering, where the clustering is achieved by cutting a graph whose edge weight represents the affinity between two data points. In LRR, each data point is represented by a linear combination of its neighbors within the same subspace, and the coefficient \mathbf{X} is estimated by

$$\begin{aligned} \min_{\mathbf{X}, \mathbf{E}} \quad & \|\mathbf{X}\|_* + \lambda \|\mathbf{E}\|_{2,1}, \\ \text{s.t.} \quad & \mathbf{D} = \mathbf{D}\mathbf{X} + \mathbf{E}. \end{aligned} \quad (46)$$

It can be shown that, if the data points in \mathbf{D} are from several orthogonal subspaces, \mathbf{X} derived from (46) will be block-diagonal [Liu et al. 2010]. Intrinsically, \mathbf{X} identifies the affinity between data points, and its block-diagonal structure indicates clusters in the data. Thus, \mathbf{X} provides a preferred affinity matrix to perform spectral clustering. A similar idea has also been applied to image segmentation [Cheng et al. 2011].

Another application of low-rank representation is in dictionary learning for classification purposes, such as detection-based visual tracking [Zhang et al. 2012b] and face recognition [Zhang et al. 2013]. In dictionary learning, the task is to construct a dictionary of atoms $\Phi = [\phi_1, \dots, \phi_n]$, such that the input signals can be represented by a linear combination of several dictionary atoms. That is $\mathbf{D} = \Phi\mathbf{X} + \mathbf{E}$, where \mathbf{X} should be sparse. In [Zhang et al. 2012b, 2013], it is claimed that \mathbf{X} should also be low-rank to learn a discriminative dictionary. The reason is that, if the constructed dictionary Φ is discriminative, the signals in \mathbf{D} with the same label should be represented by the same set of atoms in Φ . Consequently, the coefficient matrix \mathbf{X} should be a block-diagonal matrix if the columns are ordered by class labels. To impose such a structural constraint, the sparsity and the rank of \mathbf{X} are minimized simultaneously.

6.4. Image Alignment and Rectification

Image alignment is to transform different images into the same coordinate system. Peng et al. [2012] proposed to solve the problem by rank minimization based on the assumption that a batch of aligned images should form a low-rank matrix. The parameters of transformation τ were estimated by solving

$$\begin{aligned} \min_{\tau, \mathbf{X}, \mathbf{E}} \quad & \|\mathbf{X}\|_* + \lambda \|\mathbf{E}\|_1, \\ \text{s.t.} \quad & \mathbf{X} + \mathbf{E} = \mathbf{D} \circ \tau, \end{aligned} \quad (47)$$

where each column of \mathbf{D} corresponds to an image to be aligned and $\mathbf{D} \circ \tau$ denotes the images after transformation. The sparse component \mathbf{E} is to model local differences between different images.

Similarly, Zhang et al. [2012c] applied the model in (47) to generate transform-invariant low-rank textures (TILT). The difference compared to [Peng et al. 2012] is that \mathbf{D} in TILT represents a single image instead of an image sequence. The assumption of TILT is that the rectified images of textures such as characters, bar codes and urban scenes are usually symmetric patterns and consequently form low-rank matrices. The reconstructed low-rank texture can be further used in many applications such as camera calibration, 3D reconstruction, character recognition, etc.

6.5. Motion Analysis

The low-rank matrix factorization has been widely used to analyze the tracks of feature points in a video since the seminal work by Tomasi and Kanade [1992]. The key observation is that a measurement matrix composed of feature tracks will be rank-limited and the rank depends on the type of camera model (e.g. affine or perspective) and the complexity of object motion (e.g. rigid or non-rigid). For example, under the weak-perspective model, the 2D image coordinates $\mathbf{x} \in \mathbb{R}^2$ and the 3D position $X \in \mathbb{R}^3$ of a feature point are related by the following equation [Szeliski 2010]:

$$\mathbf{x} = \mathbf{M} \begin{bmatrix} X \\ 1 \end{bmatrix}, \quad (48)$$

where $\mathbf{M} \in \mathbb{R}^{2 \times 4}$ is an affine motion matrix. If a set of feature points on a rigid object are tracked across many frames, we have

$$\underbrace{\begin{bmatrix} \mathbf{x}_{11} & \cdots & \mathbf{x}_{1n} \\ \vdots & \ddots & \vdots \\ \mathbf{x}_{m1} & \cdots & \mathbf{x}_{mn} \end{bmatrix}}_{\mathbf{P} \in \mathbb{R}^{2m \times n}} = \underbrace{\begin{bmatrix} \mathbf{M}_1 \\ \vdots \\ \mathbf{M}_m \end{bmatrix}}_{\mathbf{M} \in \mathbb{R}^{2m \times 4}} \underbrace{\begin{bmatrix} X_1 & \cdots & X_n \\ 1 & \cdots & 1 \end{bmatrix}}_{\mathbf{S} \in \mathbb{R}^{4 \times n}}, \quad (49)$$

where \mathbf{x}_{ij} denotes the 2D image coordinates of point j in frame i , M_i is the affine motion matrix for frame i , and X_j is the 3D coordinates of point j . \mathbf{P} is often called the measurement matrix, \mathbf{M} is called the motion matrix, and \mathbf{S} is called the structure matrix [Tomasi and Kanade 1992]. Since the smallest dimension of \mathbf{M} is 4, we have $\text{rank}(\mathbf{P}) \leq 4$. Moreover, it is possible to recover the 3D coordinates (structure) from the 2D measurements (motion) by the factorization in (49), which is named structure from motion [Szeliski 2010]. Various approaches have been developed [Bregler et al. 2000; Irani 2002; Angst et al. 2011]. Also, the low-rank constraint could be used to help recover the feature tracks from noisy or incomplete measurements [Torresani and Bregler 2002].

Another related application is motion segmentation [Vidal and Ma 2004; Rao et al. 2010; Vidal 2011], where the feature tracks are from multiple moving objects instead of a single rigid object. The task is to segment the feature tracks into different groups. Each group of tracks belong to a single moving object. As discussed above, each group of tracks should form a rank-4 subspace. Therefore, the motion segmentation problem can be formulated as subspace clustering, i.e. dividing the feature tracks into multiple clusters with each cluster forming a low-dimensional subspace. For more introduction to subspace clustering, please refer to [Vidal 2011].

6.6. Restoration and Denoising

A popular application of matrix completion is image restoration. In some cases, it is desired to reconstruct the lost or corrupted parts of an image, which might be caused by texts or logos superposed on the image. This process is named image restoration or inpainting [Bertalmio et al. 2000]. As a natural image is approximately low-rank [Zhang et al. 2012a], the problem of restoring the corrupted pixels can be formulated as



Fig. 5. Using matrix completion for image restoration. Top: the input image with 50% missing pixels and the recovered image. Bottom: the input image corrupted by text and the recovered image. The SOFT-IMPUTE [Mazumder et al. 2010] algorithm was applied.

a matrix completion problem. Figure 5 is an illustration of using matrix completion to restore an image from randomly sampled pixels or a text-occluded image. Liang et al. [2012] used a more sophisticated model, where the texture to be recovered is modeled as both low-rank and sparse in certain transformed domain. Moreover, they assumed that the corrupted regions might be unknown and used a sparse error term to model and detect the corrupted regions. Ji et al. [2010] proposed a method for video restoration. The unreliable pixels in the video are first detected and labeled as missing. Then, the image patches are grouped such that the patches in each group share a similar underlying structure and form a low-rank matrix approximately. Finally, the matrix completion is carried out on each patch group to restore the images.

Similarly, the low-rank assumption is often used to model the coherence of multiple images for noise removal in medical image analysis. In denoising of magnetic resonance (MR) images, for example, an image sequence usually consists of multiple echo images [Bydder and Du 2006], frames of dynamic imaging [Nguyen et al. 2011] or different diffusion-weighted images [Lam et al. 2012]. While the images are different, the desired signals in these images are supposed to be correlated and consequently can be reconstructed with several significant principal components. The remaining components correspond to random noise, which are removed. Recently, Candes et al. [2013] used the SVT operator in (11) instead of classical PCA to achieve more robust results for image denoising. More importantly, it has been shown that the optimal threshold for SVT can be obtained theoretically based on the Stein's unbiased risk es-

timate [Candes et al. 2013], which brings great convenience to practical applications. The drawback of these methods is the possibility of removing image details that cannot be modeled as low-rank.

6.7. Shapes and Contours

The active shape model [Cootes et al. 1995] was proposed to increase the robustness of the deformable models for image segmentation. It constructs a statistical shape space from a large set of given shapes and constrains the candidate shape in this shape space. Suppose a vector $\mathcal{C} = [x_1, \dots, x_p, y_1, \dots, y_p]^T \in \mathbb{R}^{2p}$ represents a digitized parametric curve in the 2-D plane, where (x_i, y_i) represents a landmark point on the curve. In the active shape model, a candidate shape is represented as

$$\mathcal{C}(\mathbf{w}) = \bar{\mathcal{C}} + \Phi \mathbf{w}, \quad (50)$$

where $\bar{\mathcal{C}}$ is the mean shape, $\Phi \in \mathbb{R}^{2p \times r}$ is a matrix consisting of vectors describing shape variations in the training data, and \mathbf{w} is a vector of coefficients to represent the candidate shape in the shape space. Then, \mathbf{w} is determined by fitting the parametric curve in (50) to the features in the image. Since the number of columns of Φ is often small, the candidate shape is limited in a low-dimensional space. Hence, the active shape model intrinsically admits a low-rank assumption on the population of candidate shapes. Moreover, $\bar{\mathcal{C}}$ and Φ are derived by applying PCA to the set of training shapes.

Another way to use the low-rank constraint is to impose group-similarity constraint on multiple active contours [Zhou et al. 2013a]. When object shapes are similar, it can be shown that the shape matrix $[\mathcal{C}_1, \dots, \mathcal{C}_n]$ would be low-rank regardless of global transformation such as displacement, rotation and scaling between the shapes. Therefore, the low-rank constraint can be used to keep the shape consistency when using multiple active contours to segment a series of related images such as an echocardiographic sequence, in which the object shapes should be similar. It has been shown that such a similarity constraint can improve the robustness of the active contour model against local image defects such as missing boundaries.

6.8. Medical Image Reconstruction

Image reconstruction based on low-rank modeling has drawn much attention in the medical imaging community. The idea is to make use of the temporal coherence in dynamic imaging to reduce the required number of sampling. In MR imaging, for example, Liang [2007] proposed the concept of partial separability (PS) to model a spatial-temporal MR image $\rho(\mathbf{x}, t)$ as

$$\rho(\mathbf{x}, t) = \sum_{\ell=1}^L \phi_{\ell}(\mathbf{x})v_{\ell}(t), \quad (51)$$

where $\phi_{\ell}(\mathbf{x})$ and $v_{\ell}(t)$ for $\ell = 1, \dots, L$ are spatial and temporal components, respectively. L is the order of the model. Correspondingly, any sample in the (\mathbf{k}, t) -space can be expressed as $c(\mathbf{k}, t) = \sum_{\ell=1}^L u_{\ell}(\mathbf{k})v_{\ell}(t)$, where $u_{\ell}(\mathbf{k})$ is the Fourier transform of $\phi_{\ell}(\mathbf{x})$. Using matrix notations, we have

$$\mathbf{C} = \mathbf{U}\mathbf{V}, \quad (52)$$

where $C_{ij} = c(\mathbf{k}_i, t_j)$, $U_{i\ell} = u_{\ell}(\mathbf{k}_i)$ and $V_{\ell j} = v_{\ell}(t_j)$. Since the images are temporally coherent, L can be very small, which gives a low-rank model of the coefficients \mathbf{C} in the (\mathbf{k}, t) -space. Hence, a small number of samples are sufficient to estimate \mathbf{C} and reconstruct the image sequence. For example, $u_{\ell}(\mathbf{k})$ and $v_{\ell}(t)$ for $\ell = 1, \dots, L$ can be obtained by fully sampling L columns and rows of the (\mathbf{k}, t) -space [Liang 2007]. An

alternative approach is randomly sampling the (k, t) -space followed by solving the matrix completion problem.

The basic PS model can be further extended to integrate other sparse properties in specific domains. For example, the spatial component $\phi_\ell(\mathbf{x})$ (image intensity) often has a sparse representation in wavelets or a limited total variation [Lustig et al. 2008; Lingala et al. 2011; Majumdar and Ward 2012]. Moreover, the temporal component $v_\ell(t)$ is usually periodic or bandlimited, which results in sparsity in the Fourier domain [Zhao et al. 2010, 2012]. Also, the low-rank property can be modeled to be regionally dependent [Christodoulou et al. 2012]. Instead of using the PS model, some works [Lingala et al. 2011; Majumdar and Ward 2012] impose the low-rank property by nuclear norm minimization, which gives convex formulations. Similar methods based on low-rank modeling have also been applied to image reconstruction for other modalities such as computed tomography (CT) [Cai et al. 2012; Gao et al. 2011] and positron emission tomography (PET) [Rahmim et al. 2009].

6.9. Other Applications

Other applications of low-rank modeling include saliency detection [Shen and Wu 2012], correspondence estimation [Zeng et al. 2012, 2013], parsing façade [Yang et al. 2012], and model fusion [Ye et al. 2012], to name a few.

7. DISCUSSIONS

This paper has reviewed the concept of low-rank modeling, the representative low-rank models, the state-of-the-art algorithms, and the applications in image analysis-related areas.

The convex programming-based methods for low-rank matrix recovery generally achieve stable performance under a wide range of scenarios due to the global optimality in optimization. In noiseless cases, convex programs such as (5) and (8) can exactly recover the low-rank matrix with theoretical proofs [Candès and Recht 2009; Candès et al. 2011]. A possible drawback of convex methods is that the convex relaxation may shrink true signals or introduce bias into original models. For instance, the nuclear norm minimization will prefer a matrix with values close to zero. To compensate for the shrinkage effect, some postprocessing steps may be used [Mazumder et al. 2010]. Some other works tried to alleviate this issue by going beyond the nuclear norm and using other relaxation techniques [Mohan and Fazel 2010; Zhang et al. 2012a]. Also, the ℓ_1 -penalty may not be robust enough to remove the influence of outliers when the outlier density is relatively high [Zhou et al. 2013b; Wang and Yeung 2013]. Another notable drawback of convex methods is the requirement of repeated SVD computation in iterations, which is time consuming and unaffordable in large-scale problems. While many efforts have been made towards fast SVD computation such as partial SVD [Lin et al. 2010], approximate SVD [Ma et al. 2011] or performing SVT without SVD [Cai and Osher 2010], the speed is still too slow in many real applications. More efficient algorithms are still desired.

The matrix factorization-based methods are more popularly used in real applications (such as recommender systems [Koren et al. 2009]), mostly due to its computational convenience. Repetitively calculating SVD of a large matrix in nuclear norm minimization is replaced by updating two smaller factor matrices in matrix factorization. The loss functions in matrix factorization are usually differentiable and can be efficiently minimized by gradient-based algorithms. Moreover, the loss function is often decomposable as a sum of separate functions over data points or variables. Therefore, it is convenient to develop online algorithms for real-time processing and to design distributed algorithms for solving large-scale problems. Another advantage of matrix factorization-based methods is that they seldom introduce bias into the model, which

might be the main reason for their better performance. The foremost drawback of matrix factorization is that the optimization problem is nonconvex. Also, the matrix rank needs to be predefined in many models. These difficulties may be relieved by using Bayesian methods. However, sufficient sampling is required to globally solve a Bayesian model, which increases the computation. Hence, a tradeoff has to be made between model optimality and computational efficiency.

The low-rank modeling is based on the fact that coherence often exists among data. Such prior knowledge can be used for many purposes such as extracting common patterns, removing random noise, reducing sampling rates in image acquisition, etc. Recent progresses in sparse learning and optimization provide powerful frameworks and techniques to conveniently model the low-rank property of data and develop new algorithms. We expect to see more applications of low-rank modeling in the near future. However, it is necessary to validate the low-rank assumption for specific problems before using low-rank models.

REFERENCES

- R. Angst, C. Zach, and M. Pollefeys. The generalized trace-norm and its application to structure-from-motion problems. In *Proceedings of IEEE International Conference on Computer Vision*, 2011.
- S. D. Babacan, M. Luessi, R. Molina, and A. K. Katsaggelos. Sparse Bayesian methods for low-rank matrix estimation. *IEEE Transactions on Signal Processing*, 60(8):3964–3977, 2012.
- L. Balzano, R. Nowak, and B. Recht. Online identification and tracking of subspaces from highly incomplete information. In *Proceedings of Annual Allerton Conference on Communication, Control, and Computing*, 2010.
- R. Basri and D. Jacobs. Lambertian reflectance and linear subspaces. *IEEE Transactions on Pattern Analysis and Machine Intelligence*, 25(2):218–233, 2003.
- A. Beck and M. Teboulle. A fast iterative shrinkage-thresholding algorithm for linear inverse problems. *SIAM Journal on Imaging Sciences*, 2(1):183–202, 2009.
- M. Bertalmio, G. Sapiro, V. Caselles, and C. Ballester. Image inpainting. In *Proceedings of Annual Conference on Computer Graphics and Interactive Techniques*, 2000.
- D. Bertsekas. *Nonlinear programming*. Athena Scientific, 1999.
- C. M. Bishop. Bayesian PCA. In *Advances in Neural Information Processing Systems*, pages 382–388, 1999.
- C. M. Bishop et al. *Pattern recognition and machine learning*. Springer New York, 2006.
- A. Blake and M. Isard. *Active contours*. Springer, 2000.
- T. Blumensath and M. E. Davies. Iterative hard thresholding for compressed sensing. *Applied and Computational Harmonic Analysis*, 27(3):265–274, 2009.
- N. Boumal and P.-A. Absil. RTRMC: A Riemannian trust-region method for low-rank matrix completion. In *Advances in Neural Information Processing Systems*, pages 406–414, 2011.
- S. Boyd. Distributed optimization and statistical learning via the alternating direction method of multipliers. *Foundations and Trends in Machine Learning*, 3(1):1–122, 2010.
- C. Bregler, A. Hertzmann, and H. Biermann. Recovering non-rigid 3d shape from image streams. In *Proceedings of IEEE Conference on Computer Vision and Pattern Recognition*, 2000.
- A. M. Buchanan and A. W. Fitzgibbon. Damped newton algorithms for matrix factorization with missing data. In *Proceedings of IEEE Conference on Computer Vision and Pattern Recognition*, 2005.

- M. Bydder and J. Du. Noise reduction in multiple-echo data sets using singular value decomposition. *Magnetic Resonance Imaging*, 24(7):849–856, 2006.
- J. Cai, E. Candès, and Z. Shen. A singular value thresholding algorithm for matrix completion. *SIAM Journal on Optimization*, 20:1956, 2010.
- J. Cai, X. Jia, H. Gao, S. Jiang, Z. Shen, and H. Zhao. Cine cone beam CT reconstruction using low-rank matrix factorization: algorithm and a proof-of-principle study. *arXiv preprint arXiv:1204.3595*, 2012.
- J.-F. Cai and S. Osher. Fast singular value thresholding without singular value decomposition. *UCLA CAM Report*, 5, 2010.
- E. Candès and Y. Plan. Matrix completion with noise. *Proceedings of IEEE*, 98(6):925–936, 2010.
- E. Candès and B. Recht. Exact matrix completion via convex optimization. *Foundations of Computational Mathematics*, 9(6):717–772, 2009.
- E. Candès, X. Li, Y. Ma, and J. Wright. Robust principal component analysis? *Journal of the ACM*, 58(3):11, 2011.
- E. Candès, C. Sing-Long, and J. Trzasko. Unbiased risk estimates for singular value thresholding and spectral estimators. *IEEE Transactions on Signal Processing*, 61(19):4643–4657, 2013.
- V. Chandrasekaran, S. Sanghavi, P. Parrilo, and A. Willsky. Rank-sparsity incoherence for matrix decomposition. *SIAM Journal on Optimization*, 21(2):572–596, 2011.
- C. Chen, C. Wei, and Y. Wang. Low-rank matrix recovery with structural incoherence for robust face recognition. In *Proceedings of IEEE Conference on Computer Vision and Pattern Recognition*, 2012.
- P. Chen. Optimization algorithms on subspaces: Revisiting missing data problem in low-rank matrix. *International Journal of Computer Vision*, 80(1):125–142, 2008.
- B. Cheng, G. Liu, J. Wang, Z. Huang, and S. Yan. Multi-task low-rank affinity pursuit for image segmentation. In *Proceedings of IEEE International Conference on Computer Vision*, 2011.
- A. Christodoulou, S. Babacan, and Z. Liang. Accelerating cardiovascular imaging by exploiting regional low-rank structure via group sparsity. In *Proceedings of IEEE International Symposium on Biomedical Imaging*, 2012.
- T. Cootes, C. Taylor, D. Cooper, and J. Graham. Active shape models – their training and application. *Computer Vision and Image Understanding*, 61(1):38–59, 1995.
- X. Cui, J. Huang, S. Zhang, and D. N. Metaxas. Background subtraction using low rank and group sparsity constraints. In *Proceedings of European Conference on Computer Vision*, 2012.
- W. Dai and O. Milenkovic. SET: an algorithm for consistent matrix completion. In *Proceedings of IEEE International Conference on Acoustics Speech and Signal Processing*, 2010.
- F. De La Torre and M. Black. A framework for robust subspace learning. *International Journal of Computer Vision*, 54(1):117–142, 2003.
- X. Ding, L. He, and L. Carin. Bayesian robust principal component analysis. *IEEE Transactions on Image Processing*, 20(12):3419–3430, 2011.
- G. Doretto, A. Chiuso, Y. Wu, and S. Soatto. Dynamic textures. *International Journal of Computer Vision*, 51(2):91–109, 2003.
- C. Eckart and G. Young. The approximation of one matrix by another of lower rank. *Psychometrika*, 1(3):211–218, 1936.
- M. Fazel. *Matrix rank minimization with applications*. PhD thesis, Stanford University, 2002.
- H. Gao, J. Cai, Z. Shen, and H. Zhao. Robust principal component analysis-based four-dimensional computed tomography. *Physics in Medicine and Biology*, 56(11):3181, 2011.

- Z. Gao, L. Cheong, and M. Shan. Block-sparse RPCA for consistent foreground detection. In *Proceedings of European Conference on Computer Vision*, 2012.
- R. Gemulla, E. Nijkamp, P. J. Haas, and Y. Sismanis. Large-scale matrix factorization with distributed stochastic gradient descent. In *Proceedings of International Conference on Knowledge Discovery and Data Mining*, 2011.
- A. S. Georghiadis, P. N. Belhumeur, and D. J. Kriegman. From few to many: Illumination cone models for face recognition under variable lighting and pose. *IEEE Transactions on Pattern Analysis and Machine Intelligence*, 23(6):643–660, 2001.
- J. He, L. Balzano, and A. Szlam. Incremental gradient on the grassmannian for online foreground and background separation in subsampled video. In *Proceedings of IEEE Conference on Computer Vision and Pattern Recognition*, 2012.
- H. Hotelling. Analysis of a complex of statistical variables into principal components. *The Journal of Educational Psychology*, pages 498–520, 1933.
- M. Irani. Multi-frame correspondence estimation using subspace constraints. *International Journal of Computer Vision*, 48(3):173–194, 2002.
- P. Jain, R. Meka, and I. S. Dhillon. Guaranteed rank minimization via singular value projection. In *Proceedings of Advances in Neural Information Processing Systems*, 2010.
- H. Ji, C. Liu, Z. Shen, and Y. Xu. Robust video denoising using low rank matrix completion. In *Proceedings of IEEE Conference on Computer Vision and Pattern Recognition*, pages 1791–1798, 2010.
- S. Ji and J. Ye. An accelerated gradient method for trace norm minimization. In *Proceedings of International Conference on Machine Learning*, 2009.
- I. T. Jolliffe. *Principal component analysis*. Springer verlag, 2002.
- Q. Ke and T. Kanade. Robust l1 norm factorization in the presence of outliers and missing data by alternative convex programming. In *Proceedings of IEEE Conference on Computer Vision and Pattern Recognition*, 2005.
- R. H. Keshavan, A. Montanari, and S. Oh. Low-rank matrix completion with noisy observations: a quantitative comparison. In *Proceedings of Annual Allerton Conference on Communication, Control, and Computing*, 2009.
- R. H. Keshavan, A. Montanari, and S. Oh. Matrix completion from a few entries. *IEEE Transactions on Information Theory*, 56(6):2980–2998, 2010.
- M. Kirby and L. Sirovich. Application of the Karhunen-Loeve procedure for the characterization of human faces. *IEEE Transactions on Pattern Analysis and Machine Intelligence*, 12(1):103–108, 1990.
- Y. Koren, R. Bell, and C. Volinsky. Matrix factorization techniques for recommender systems. *Computer*, 42(8):30–37, 2009.
- B. Lakshminarayanan, G. Bouchard, and C. Archambeau. Robust Bayesian matrix factorisation. In *International Conference on Artificial Intelligence and Statistics*, pages 425–433, 2011.
- F. Lam, S. Babacan, J. Haldar, N. Schuff, and Z. Liang. Denoising diffusion-weighted MR magnitude image sequences using low rank and edge constraints. In *Proceedings of IEEE International Symposium on Biomedical Imaging*, 2012.
- N. Lawrence. Probabilistic non-linear principal component analysis with Gaussian process latent variable models. *The Journal of Machine Learning Research*, 6:1783–1816, 2005.
- D. Lee and H. Seung. Learning the parts of objects by non-negative matrix factorization. *Nature*, 401(6755):788, 1999.
- K. Lee and Y. Bresler. Admira: Atomic decomposition for minimum rank approximation. *IEEE Transactions on Information Theory*, 56(9):4402–4416, 2010.
- L. Li, W. Huang, I. Gu, and Q. Tian. Statistical modeling of complex backgrounds for foreground object detection. *IEEE Transactions Image Processing*, 13(11):1459–

- 1472, 2004.
- X. Liang, X. Ren, Z. Zhang, and Y. Ma. Repairing sparse low-rank texture. In *Proceedings of European conference on Computer Vision*, 2012.
- Z. Liang. Spatiotemporal imaging with partially separable functions. In *Proceedings of IEEE International Symposium on Biomedical Imaging*, 2007.
- Z. Lin, M. Chen, and Y. Ma. The augmented Lagrange multiplier method for exact recovery of corrupted low-rank matrices. *arXiv preprint arXiv:1009.5055*, 2010.
- S. Lingala, Y. Hu, E. DiBella, and M. Jacob. Accelerated dynamic MRI exploiting sparsity and low-rank structure: kt SLR. *IEEE Transactions on Medical Imaging*, 30(5):1042–1054, 2011.
- G. Liu, Z. Lin, and Y. Yu. Robust subspace segmentation by low-rank representation. In *Proceedings of International Conference on Machine Learning*, 2010.
- M. Lustig, D. Donoho, J. Santos, and J. Pauly. Compressed sensing MRI. *IEEE Signal Processing Magazine*, 25(2):72–82, 2008.
- S. Ma, D. Goldfarb, and L. Chen. Fixed point and bregman iterative methods for matrix rank minimization. *Mathematical Programming*, 128(1-2):321–353, 2011.
- D. J. MacKay. Probable networks and plausible predictions—a review of practical Bayesian methods for supervised neural networks. *Network: Computation in Neural Systems*, 6(3):469–505, 1995.
- A. Majumdar and R. Ward. Exploiting rank deficiency and transform domain sparsity for MR image reconstruction. *Magnetic Resonance Imaging*, 30(1):9–18, 2012.
- S. G. Mallat and Z. Zhang. Matching pursuits with time-frequency dictionaries. *IEEE Transactions on Signal Processing*, 41(12):3397–3415, 1993.
- I. Markovsky. *Low rank approximation: algorithms, implementation, applications*. Springer, 2012.
- R. Mazumder, T. Hastie, and R. Tibshirani. Spectral regularization algorithms for learning large incomplete matrices. *The Journal of Machine Learning Research*, 11: 2287–2322, 2010.
- M. Michenková. Numerical algorithms for low-rank matrix completion problems, 2011.
- K. Mohan and M. Fazel. Iterative reweighted least squares for matrix rank minimization. In *Proceedings of Annual Allerton Conference on Communication, Control, and Computing*, 2010.
- J. Moreau. Proximité et dualité dans un espace hilbertien. *Bulletin de la Société Mathématique de France*, 93(2):273–299, 1965.
- D. Needell and J. A. Tropp. Cosamp: Iterative signal recovery from incomplete and inaccurate samples. *Applied and Computational Harmonic Analysis*, 26(3):301–321, 2009.
- Y. Nesterov. A method of solving a convex programming problem with convergence rate $O(1/k^2)$. In *Sov. Math., Dokl.*, volume 27, pages 372–376, 1983.
- Y. Nesterov. Gradient methods for minimizing composite objective function. Technical report, Université catholique de Louvain, Center for Operations Research and Econometrics (CORE), 2007.
- H. Nguyen, X. Peng, M. Do, and Z. Liang. Spatiotemporal denoising of MR spectroscopic imaging data by low-rank approximations. In *Proceedings of IEEE International Symposium on Biomedical Imaging*, 2011.
- B. O’Donoghue and E. Candes. Adaptive restart for accelerated gradient schemes. *arXiv preprint arXiv:1204.3982*, 2012.
- T. Okatani and K. Deguchi. On the Wiberg algorithm for matrix factorization in the presence of missing components. *International Journal of Computer Vision*, 72(3): 329–337, 2007.
- T. Okatani, T. Yoshida, and K. Deguchi. Efficient algorithm for low-rank matrix factorization with missing components and performance comparison of latest algorithms.

- In *Proceedings of IEEE International Conference on Computer Vision*, 2011.
- N. Oliver, B. Rosario, and A. Pentland. A Bayesian computer vision system for modeling human interactions. *IEEE Transactions on Pattern Analysis and Machine Intelligence*, 22(8):831–843, 2000.
- Y. Peng, A. Ganesh, J. Wright, W. Xu, and Y. Ma. Rasl: Robust alignment by sparse and low-rank decomposition for linearly correlated images. *IEEE Transactions on Pattern Analysis and Machine Intelligence*, 34(11):2233–2246, 2012.
- A. Rahmim, J. Tang, and H. Zaidi. Four-dimensional (4D) image reconstruction strategies in dynamic PET: beyond conventional independent frame reconstruction. *Medical physics*, 36:3654, 2009.
- S. Rao, R. Tron, R. Vidal, and Y. Ma. Motion segmentation in the presence of outlying, incomplete, or corrupted trajectories. *IEEE Transactions on Pattern Analysis and Machine Intelligence*, 32(10):1832–1845, 2010.
- B. Recht and C. Ré. Parallel stochastic gradient algorithms for large-scale matrix completion. *Mathematical Programming Computation*, pages 1–26, 2011.
- B. Recht, M. Fazel, and P. Parrilo. Guaranteed minimum-rank solutions of linear matrix equations via nuclear norm minimization. *SIAM Review*, 52(3):471–501, 2010.
- J. Rennie and N. Srebro. Fast maximum margin matrix factorization for collaborative prediction. In *Proceedings of International Conference on Machine Learning*, 2005.
- R. Salakhutdinov and A. Mnih. Bayesian probabilistic matrix factorization using markov chain monte carlo. In *Proceedings of International Conference on Machine Learning*, 2008a.
- R. Salakhutdinov and A. Mnih. Probabilistic matrix factorization. In *Advances in Neural Information Processing Systems*, 2008b.
- X. Shen and Y. Wu. A unified approach to salient object detection via low rank matrix recovery. In *Proceedings of IEEE Conference on Computer Vision and Pattern Recognition*, 2012.
- H.-Y. Shum, K. Ikeuchi, and R. Reddy. Principal component analysis with missing data and its application to polyhedral object modeling. *IEEE Transactions on Pattern Analysis and Machine Intelligence*, 17(9):854–867, 1995.
- A. P. Singh and G. J. Gordon. A unified view of matrix factorization models. In *Machine Learning and Knowledge Discovery in Databases*, pages 358–373. Springer, 2008.
- L. Sirovich and M. Kirby. Low-dimensional procedure for the characterization of human faces. *Journal of the Optical Society of America. A, Optics and image science*, 4(3):519–524, 1987.
- N. Srebro, J. Rennie, and T. Jaakkola. Maximum-margin matrix factorization. *Advances in Neural Information Processing Systems*, 17(5):1329–1336, 2005.
- R. Szeliski. *Computer vision: algorithms and applications*. Springer-Verlag, 2010.
- M. E. Tipping. Sparse Bayesian learning and the relevance vector machine. *The Journal of Machine Learning Research*, 1:211–244, 2001.
- M. E. Tipping and C. M. Bishop. Probabilistic principal component analysis. *Journal of the Royal Statistical Society: Series B (Statistical Methodology)*, 61(3):611–622, 1999.
- K. Toh and S. Yun. An accelerated proximal gradient algorithm for nuclear norm regularized linear least squares problems. *Pacific Journal of Optimization*, 6(615-640):15, 2010.
- C. Tomasi and T. Kanade. Shape and motion from image streams under orthography: a factorization method. *International Journal of Computer Vision*, 9(2):137–154, 1992.
- R. Tomioka, T. Suzuki, M. Sugiyama, and H. Kashima. A fast augmented lagrangian algorithm for learning low-rank matrices. In *Proceedings of International Conference on Machine Learning*, 2010.

- L. Torresani and C. Bregler. Space-time tracking. In *Proceedings of European Conference on Computer Vision*, 2002.
- I. Todic and P. Frossard. Dictionary learning. *IEEE Signal Processing Magazine*, 28(2):27–38, 2011.
- M. A. Turk and A. P. Pentland. Face recognition using eigenfaces. In *Proceedings of IEEE Conference on Computer Vision and Pattern Recognition*, 1991.
- R. Vidal. Subspace clustering. *IEEE Signal Processing Magazine*, 28(2):52–68, 2011.
- R. Vidal and R. Hartley. Motion segmentation with missing data using PowerFactorization and GPCA. In *Proceedings of IEEE Conference on Computer Vision and Pattern Recognition*, 2004.
- R. Vidal and Y. Ma. A unified algebraic approach to 2-D and 3-D motion segmentation. In *Proceedings of European Conference on Computer Vision*, 2004.
- N. Wang and D.-Y. Yeung. Bayesian robust matrix factorization for image and video processing. In *Proceedings of International Conference on Computer Vision*, 2013.
- N. Wang, T. Yao, J. Wang, and D.-Y. Yeung. A probabilistic approach to robust matrix factorization. In *Proceedings of European conference on Computer Vision*, 2012.
- A. E. Waters, A. C. Sankaranarayanan, and R. Baraniuk. Sparcs: Recovering low-rank and sparse matrices from compressive measurements. In *Advances in Neural Information Processing Systems*, 2011.
- Z. Wen, W. Yin, and Y. Zhang. Solving a low-rank factorization model for matrix completion by a nonlinear successive over-relaxation algorithm. *Mathematical Programming Computation*, pages 1–29, 2010.
- J. Wright, A. Ganesh, K. Min, and Y. Ma. Compressive principal component pursuit. In *Proceedings of IEEE International Symposium on Information Theory*, 2012.
- H. Xu, C. Caramanis, and S. Sanghavi. Robust pca via outlier pursuit. *IEEE Transactions on Information Theory*, 58(5):3047–3064, may 2012a.
- Y. Xu, W. Yin, Z. Wen, and Y. Zhang. An alternating direction algorithm for matrix completion with nonnegative factors. *Frontiers of Mathematics in China*, 7(2):365–384, 2012b.
- C. Yang, T. Han, L. Quan, and C. Tai. Parsing façade with rank-one approximation. In *Proceedings of IEEE Conference on Computer Vision and Pattern Recognition*, 2012.
- G. Ye, D. Liu, I. Jhuo, and S. Chang. Robust late fusion with rank minimization. In *Proceedings of IEEE Conference on Computer Vision and Pattern Recognition*, 2012.
- Z. Zeng, T.-H. Chan, K. Jia, and D. Xu. Finding correspondence from multiple images via sparse and low-rank decomposition. In *Proceedings of European Conference on Computer Vision*, 2012.
- Z. Zeng, S. Xiao, K. Jia, T.-H. Chan, S. Gao, D. Xu, and Y. Ma. Learning by associating ambiguously labeled images. In *Proceedings of IEEE Conference on Computer Vision and Pattern Recognition*, 2013.
- D. Zhang, C. Hangzhou, Y. Hu, J. Ye, X. Li, and X. He. Matrix completion by truncated nuclear norm regularization. In *Proceedings of IEEE Conference on Computer Vision and Pattern Recognition*, 2012a.
- T. Zhang, B. Ghanem, S. Liu, and N. Ahuja. Low-rank sparse learning for robust visual tracking. In *Proceedings of European Conference on Computer Vision*, pages 470–484. Springer, 2012b.
- Y. Zhang, Z. Jiang, and L. S. Davis. Learning structured low-rank representations for image classification. In *Proceedings of IEEE Conference on Computer Vision and Pattern Recognition*, 2013.
- Z. Zhang, A. Ganesh, X. Liang, and Y. Ma. TILT: Transform invariant low-rank textures. *International Journal of Computer Vision*, 99:1–24, 2012c.
- B. Zhao, J. Haldar, C. Brinegar, and Z. Liang. Low rank matrix recovery for real-time cardiac MRI. In *Proceedings of IEEE International Symposium on Biomedical*

- Imaging*, 2010.
- B. Zhao, J. Haldar, A. Christodoulou, and Z.-P. Liang. Image reconstruction from highly undersampled (k,t)-space data with joint partial separability and sparsity constraints. *IEEE Transactions on Medical Imaging*, 31(9):1809–1820, 2012.
- T. Zhou and D. Tao. Godec: Randomized low-rank & sparse matrix decomposition in noisy case. In *Proceedings of International Conference on Machine Learning*, 2011.
- X. Zhou and W. Yu. Low-rank modeling and its applications in medical image analysis. In *Proceedings of SPIE Defense, Security, and Sensing*, 2013.
- X. Zhou, X. Huang, J. Duncan, and W. Yu. Active contours with group similarity. In *Proceedings of IEEE Conference on Computer Vision and Pattern Recognition*, 2013a.
- X. Zhou, C. Yang, and W. Yu. Moving object detection by detecting contiguous outliers in the low-rank representation. *IEEE Transactions on Pattern Analysis and Machine Intelligence*, 35(3):597–610, 2013b. .
- Z. Zhou, X. Li, J. Wright, E. Candes, and Y. Ma. Stable principal component pursuit. In *Proceedings of IEEE International Symposium on Information Theory*, 2010.